Development of the Gyrokinetic-MHD Energetic Particle Code GMEC and Initial Simulation Results

Guoyong Fu, Peiyou Jiang, Zhaoyang Liu, Shiyang Liu, Lulu Zhang, Jian Bao*

IFTS, Zhejiang University, Hangzhou, China
*Institute of Physics, CAS, Beijing, China

The 4th Trilateral International Workshop on Energetic Particle Physics
LiuTong Hotel, Hangzhou, China, Oct 26-27, 2024

Outline

- Introduction
- Gyrokinetic-MHD Hybrid Model
- Development of GMEC
- GMEC verifications
- GMEC applications
- Summary
- Future Work

Introduction

- Energetic particle (EP) physics is crucial for burning plasmas:
  - EP-driven Alfvenic modes can strongly modify alpha particle distribution and induce alpha particle losses in burning plasmas ;
  - EP can have significant effects on thermal plasmas.

- The goal of this work is development of a highly efficient code for simulating energetic particle-driven Alfven modes and energetic particle transport in burning plasmas such as ITER;

- An initial version of GMEC has been developed based on gyrokinetic-MHD hybrid model. Work is in progress for adding fluid nonlinear physics as well as applying code to present tokamak experiments and future burning plasmas.

P. Y. Jiang et al, Phys. Plasmas 31, 073904 (2024
Z.Y. Liu et al, *Phys. Plasmas* 31, 073905 (2024)

Comparison with existing hybrid codes

codes	model	type	Numerical methods
MEGA	Kinetic-MHD	hybrid	explicit， finite difference， PIC
M3D-K	Kinetic-MHD	hybrid	Semi-implicit, finite element， PIC
M3D-C1-K	Kinetic-MHD	hybrid	Semi-implicit, finite element， PIC
NIMROD	Kinetic-MHD	hybrid	Semi-implicit, finite element， PIC
CLT-K	Kinetic-MHD	hybrid	Explicit, finite difference， PIC
GMEC	Gyrokinetic-MHD	hybrid	Explicit, finite difference, PIC

Compared with existing hybrid codes, GMEC has more thermal ion kinetic physics, and is highly optimized for computational efficiency. GMEC uses field-aligned coordinates and symbolic method for coding.

Outline

- Introduction
- Gyrokinetic-MHD Hybrid Model
- Development of GMEC
- GMEC verifications
- GMEC applications
- Summary
- Future Work

Gyrokinetic MHD Hybrid Equations

$$\frac{d}{dt}\left[\frac{n_i e^2}{T_i}(1-\Gamma_0)\Phi\right]+\delta\boldsymbol{B}\cdot\nabla\frac{J_\|}{B}+(\boldsymbol{B}+\delta\boldsymbol{B})\cdot\nabla\frac{\delta J_\|}{B}$$

$$+\frac{\boldsymbol{B}\times\nabla B}{B^3}\cdot\nabla\left(\delta P_\| + \delta P_\perp\right)=0\,,$$

$$\frac{d}{dt}=\frac{\partial}{\partial t}+\left(\frac{\boldsymbol{b}\times\nabla\Phi}{B}+\boldsymbol{V}_{*i}\right)\cdot\nabla\,,$$

$$\Gamma_0=e^{-k_\perp^2\rho_i^2}\mathrm{I}_0\left(k_\perp^2\rho_i^2\right),$$

$$\frac{\partial}{\partial t}A_\| = -\nabla_\|\Phi+\frac{1}{en_e}\nabla_\| P_e\,,$$

$$\frac{d}{dt}P_e=-\gamma\nabla\cdot\boldsymbol{V}_e P_e\,,$$

$$\boldsymbol{V}_e=\frac{\boldsymbol{E}\times\boldsymbol{B}}{B^2}-\frac{\delta J_\|}{en_e}\boldsymbol{b}\,,$$

$$\frac{d\boldsymbol{X}}{dt}=\frac{1}{B^{**}}\left\{v_\|\boldsymbol{B}^*-\boldsymbol{b}\times\left[\langle\boldsymbol{E}\rangle-\frac{\mu}{q_s}\nabla\left(B+\langle\delta B\rangle\right)\right]\right\},$$

$$m_s\frac{dv_\|}{dt}=\frac{q_s}{B^{**}}\boldsymbol{B}^*\cdot\left[\langle\boldsymbol{E}\rangle-\frac{\mu}{q_s}\nabla\left(B+\langle\delta B\rangle\right)\right],$$

$$\boldsymbol{B}^*=\boldsymbol{B}+\langle\delta\boldsymbol{B}\rangle+\frac{mv_\|}{e}\nabla\times\boldsymbol{b}\,,\quad B^{**}=\boldsymbol{B}^*\cdot\boldsymbol{b}\,。$$

$$\boldsymbol{E}=-\nabla\Phi-\frac{\partial A_\|}{\partial t}\boldsymbol{b}\,,$$

$$\delta\boldsymbol{B}=\nabla\times\left(A_\|\boldsymbol{b}\right)。$$

Development of GMEC

- Field-aligned coordinates
- Discretization methods
- Compile-time Symbolic Solver (CSS)
- δf PIC method for solving the EP and thermal ion distributions
- Equilibrium interface with VMEC and DESC
- Code optimization

Field-aligned Coordinates and Meshes

- Flux coordinates (ψ,θ,φ)

- Field-aligned coordinates $x=\dfrac{\psi-\psi_1}{\Delta\psi}$，$y=\theta$，$z=\varphi-\int_{\theta_0}^{\theta}d\theta'\nu(\psi,\theta')$

$$\nu(\psi,\theta)=\boldsymbol{B}\cdot\nabla\varphi/\boldsymbol{B}\cdot\nabla\theta$$

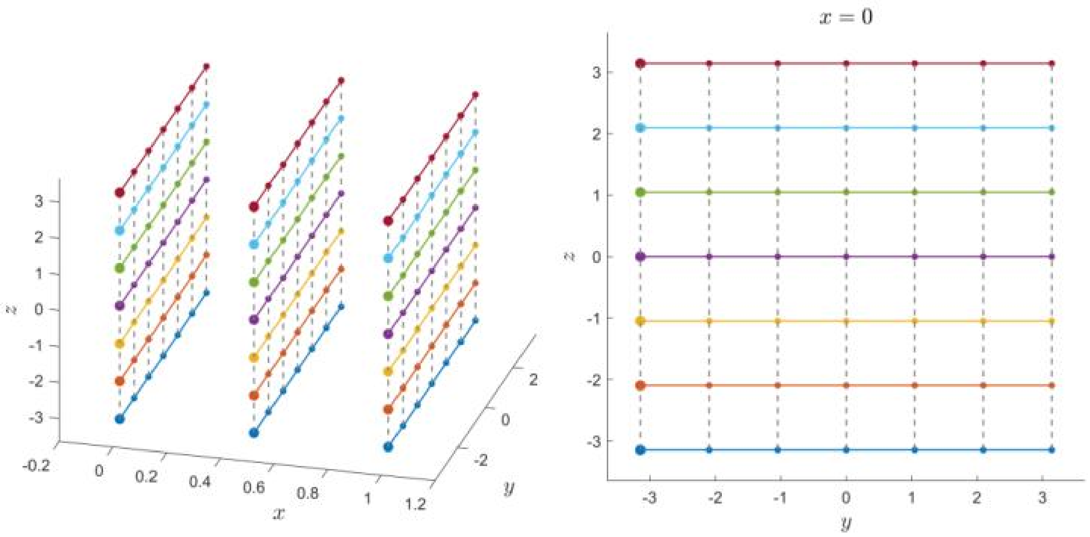

图 1.1：(x,y,z)坐标系中 3×6×6 的三维均匀网格

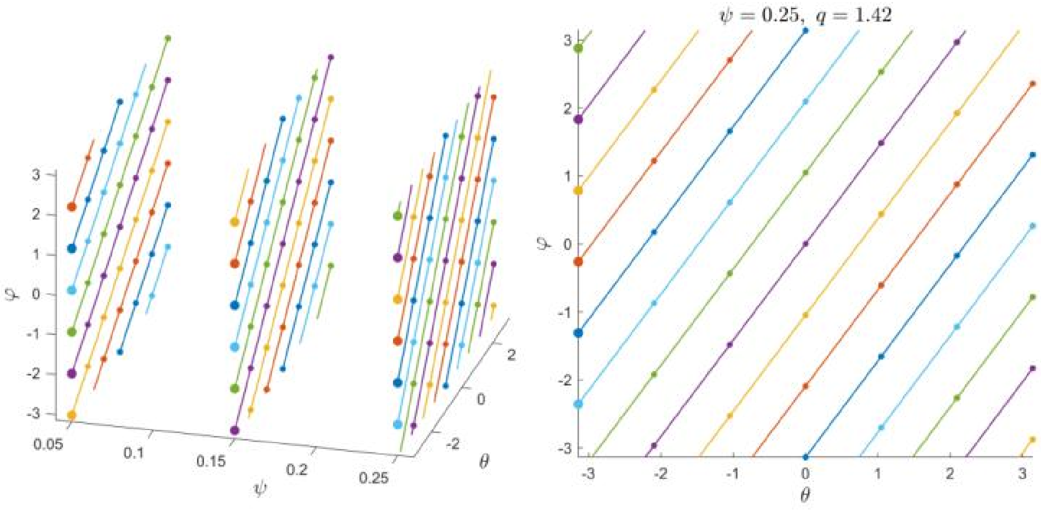

图 1.2：(ψ,θ,φ)坐标系中的磁力线覆盖整个磁面

Discretization Methods

- 4^{th} order finite difference in space (5 point central difference);

- 4^{th} order Runge Kutta method in time advance.

Compile-time Symbolic Solver (CSS)

Peiyou Jiang

Field-aligned coordinates brings the benefit that relatively few grids are needed in the parallel coordinate.

$$\nabla_{\parallel}^2 \ll \nabla_{\perp}^2$$

However, expanding equations in curvilinear coordinates suffers both numerical and physical complexities, especially with high order finite difference.

Compile-time Symbolic Solver (CSS) is developed to solve PDE and ODE in finite difference method.

CSS is a general-purpose framework. It aims to generate finite difference codes quickly and greatly reduce the risks of coding errors. Furthermore, the codes generated by CSS have better performance than conventional approaches.

CSS is a C++20 metaprogramming code. All the symbolic operations are completed at compile time.

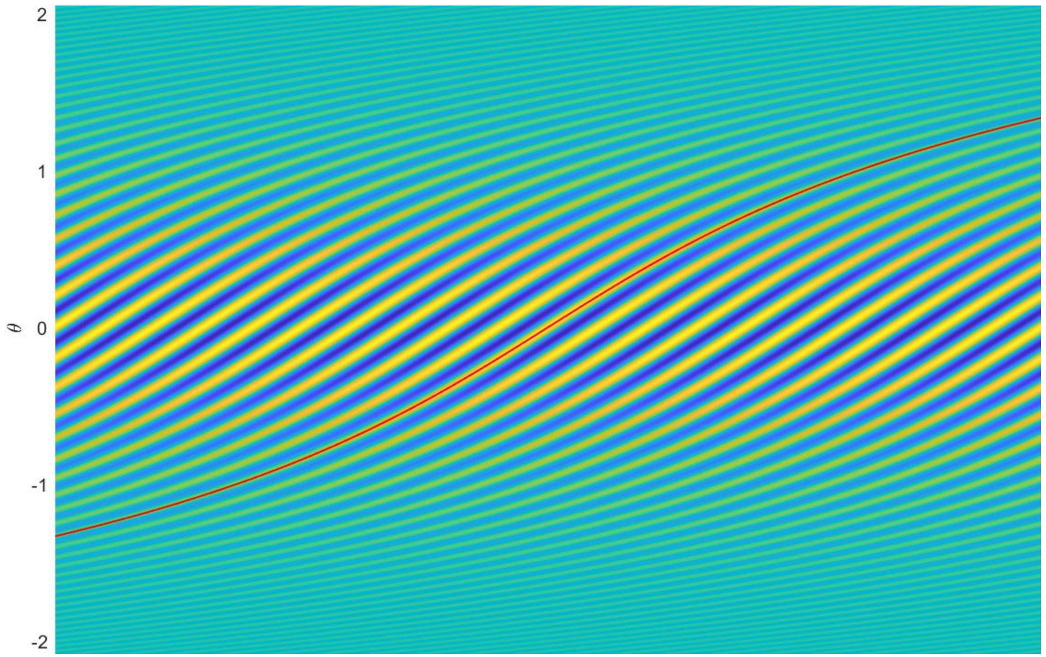

Mode structure of IBM in θ, ϕ coordinate

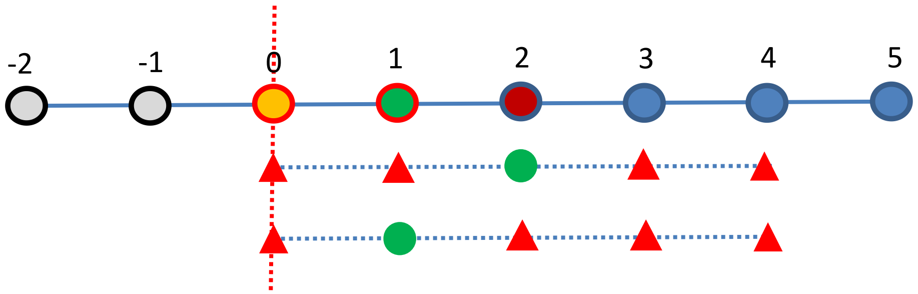

Biased difference scheme in boundary

Symbolic implementation of GMEC

$$\nabla_{\parallel} = \vec{b} \cdot \nabla$$

auto Nabla_p = b*Nabla

$$\delta\varpi = \nabla \cdot \frac{1}{v_A^2} \nabla_{\perp} \delta\Phi$$

auto dw = Div*(_va2*Nabla*dPhi)

$$\delta J_{\parallel} = -\frac{1}{B} \nabla \cdot \left(B^2 \nabla_{\perp} \left(\frac{\delta A_{\parallel}}{B} \right) \right)$$

auto dJp = - Div*(Bs2*Nabla*(dA/Bs))/Bs

$$\delta\vec{B} = \nabla \times \left(\delta A_{\parallel} \vec{b} \right)$$

auto dB = Cross(Nabla,dA*b)

$$\vec{v}_{*i} = \frac{1}{enB} \vec{b} \times \nabla \mathrm{P_i}$$

auto v_star = Cross(b,Nabla*Pi)
/(e*n*Bs)

$$\vec{v}_{E\times B} = \frac{1}{B} \vec{b} \times \nabla \delta\Phi$$

auto v_EB = Cross(b,Nabla*Phi)/Bs

$$\vec{v}_d = \frac{1}{B} \vec{b} \times \vec{\kappa}$$

auto v_d = Cross(b,kappa)/Bs

$$\frac{\partial}{\partial t} \delta\varpi = -\vec{v}_{*i} \cdot \nabla \delta\varpi \quad + \delta\vec{B} \cdot \nabla \left(\frac{\mathrm{J}_{\parallel}}{B} \right) \quad + \vec{B} \cdot \nabla \left(\frac{\delta J_{\parallel}}{B} \right) \quad + 2\vec{v}_d \cdot \nabla_{\perp} \delta P$$

```
constexpr auto dw_dt = -v_star*Nabla*dw + dB*Nabla*(Jp/Bs) + Bs*b*Nabla*(dJ/Bs) +
Ratio<2>{}*v_d*Nabla*dP
```

Interface with equilibrium codes (VMEC and DESC)

$$(R, Z, \phi) \rightarrow (\psi, \theta_V, \xi_V)/(\rho, \theta_D, \xi_D) \rightarrow (\psi, \theta_B, \xi_B) \rightarrow (x, y, z) \rightarrow (x', y', z')$$

Cylindrical VMEC/DESC Boozer Field-aligned Shifted metric

[D. W. Dudt. 2022 POP]

$$M = \frac{\partial(R, Z, \phi)}{\partial(\psi, \theta, \xi)} = \begin{bmatrix} \partial_\psi R & \partial_\theta R & 0 \\ \partial_\psi Z & \partial_\theta Z & 0 \\ 0 & 0 & 1 \end{bmatrix} \qquad g^{\psi\theta\phi} = M^{-1} g^{RZ\phi} (M^{-1})^T$$

$$M_2 = \frac{\partial(x, y, z)}{\partial(\psi, \theta, \xi)} = \begin{bmatrix} 1 & 0 & 0 \\ 0 & 1 & 0 \\ -I & -\nu & 1 \end{bmatrix} \qquad g^{xyz} = M_2 g^{\psi\theta\phi} (M_2)^T$$

$$I_s'(\psi, \theta) = \int_{\theta_i}^{\theta} \nu(\psi, \theta') d\theta'$$

$$z_0' = 0, \;\; I_s' = 0, \;\; \partial_x I_s' = 0, \;\; \partial_y I_s' = \nu$$

$\partial_\psi g^{ij}, \partial_\theta g^{ij}, \partial_\psi g_{ij}, \partial_\theta g_{ij}$

Code Flow Chart

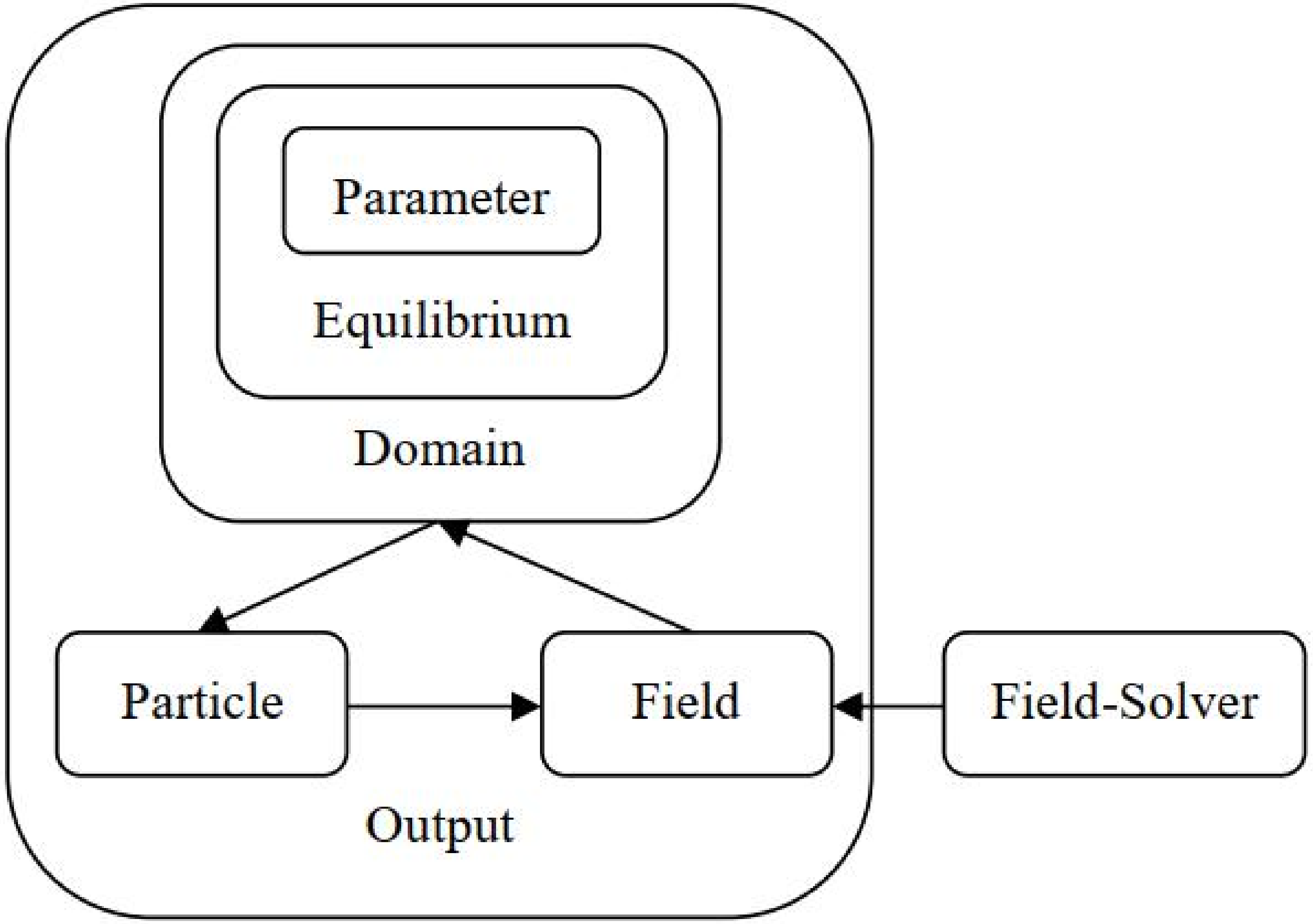

图 1.4：动理学求解模块的程序框架

Parallelization Methods

- MPI for 1D domain decomposition along magnetic field direction;

- Intel TBB (Thread Building Block) for each domain.

GMEC is highly optimized and much faster than a typical gyrokinetic code

Shiyang Liu

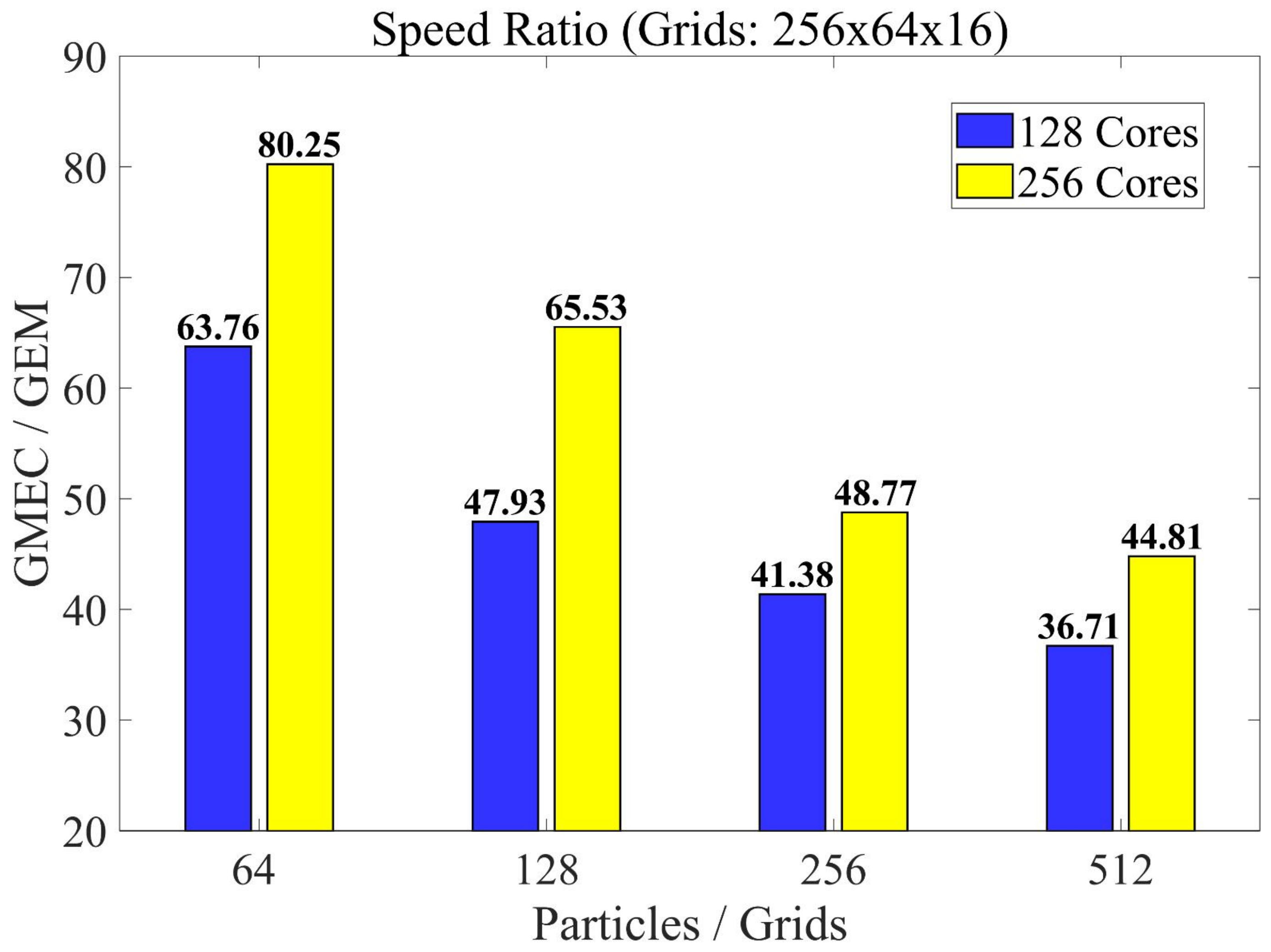

Runge-Kutta: 2 order
Gyro-Average: 4 points

A GPU version of GMEC has been developed with high efficiency

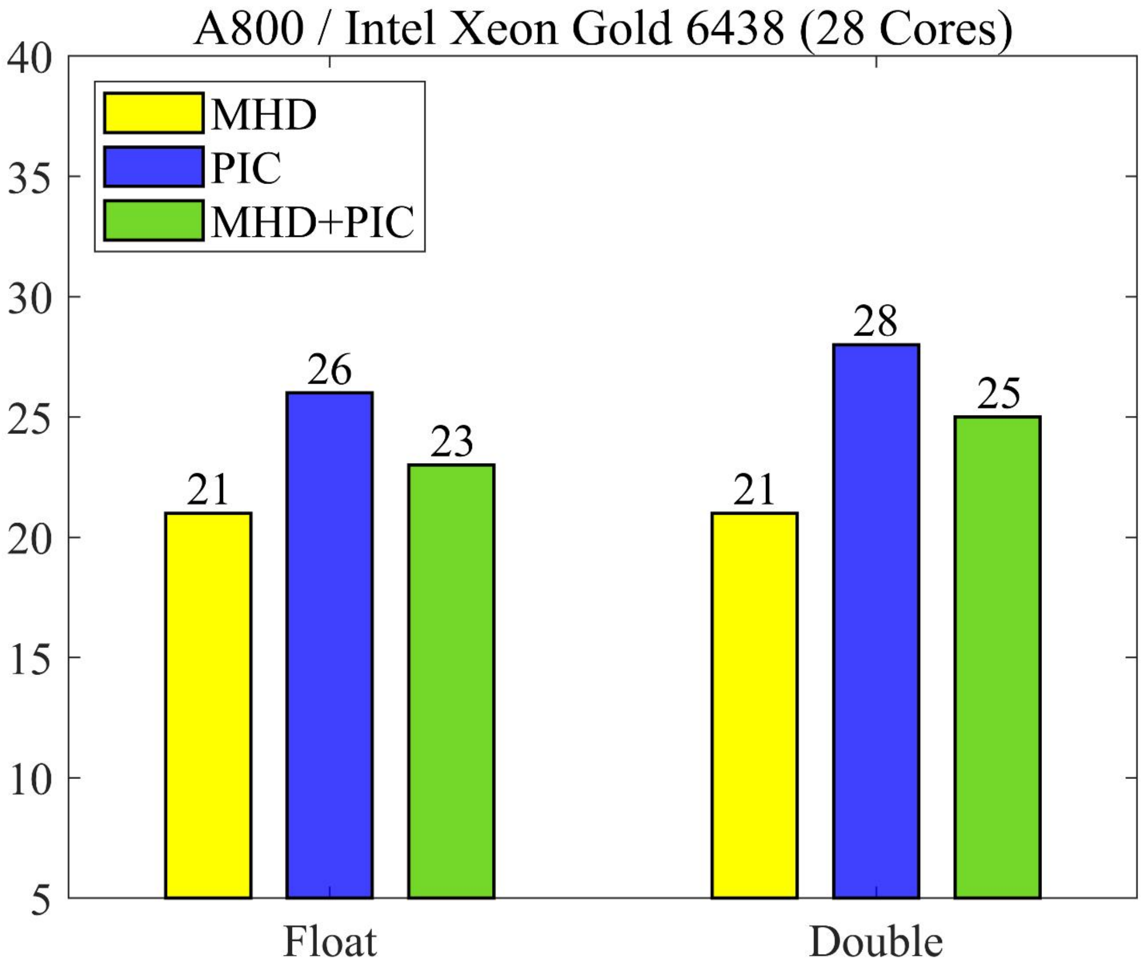

$n = 6, \; TAE, \; 256 \times 64 \times 16$

$N_p = 1.6 \times 10^7$

$dt = 0.1R_0/v_A, \mathrm{t} = 250R_0/v_A$

A800: $52.3s$

one A800 ≈ 640 cores

Shiyang Liu, poster this afternoon!

Outline

- Introduction
- Gyrokinetic-MHD Hybrid Model
- Development of GMEC
- GMEC verifications
- GMEC applications
- Summary
- Future Work

Benchmark with MAS: ideal ballooning mode

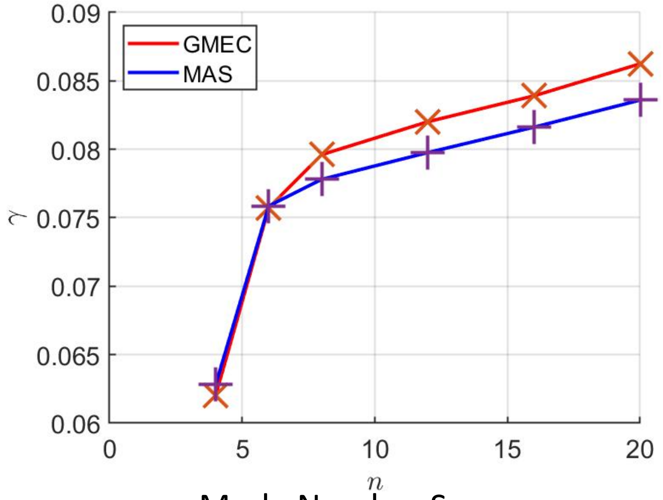

Mode Number Scan

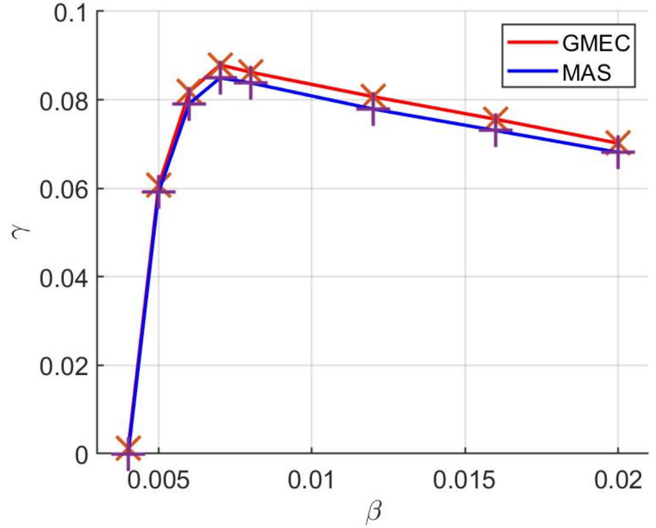

β Scan

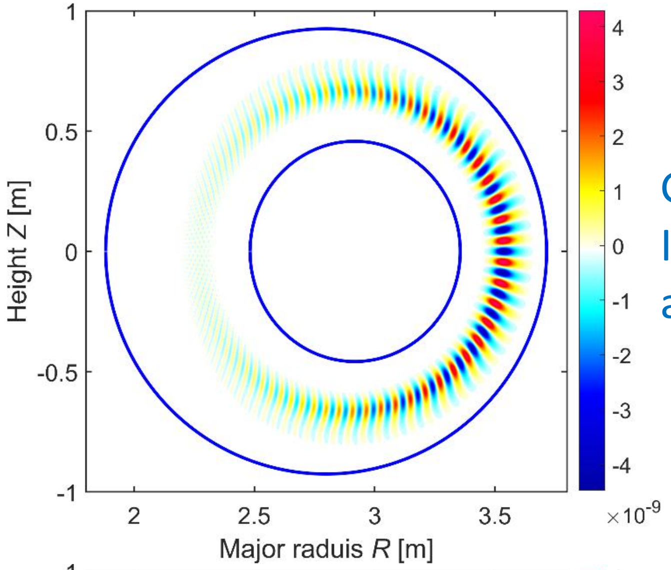

GMEC
Initial value approach

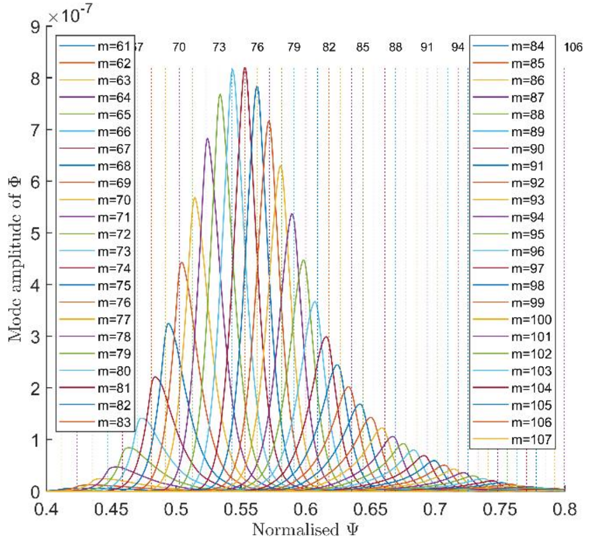

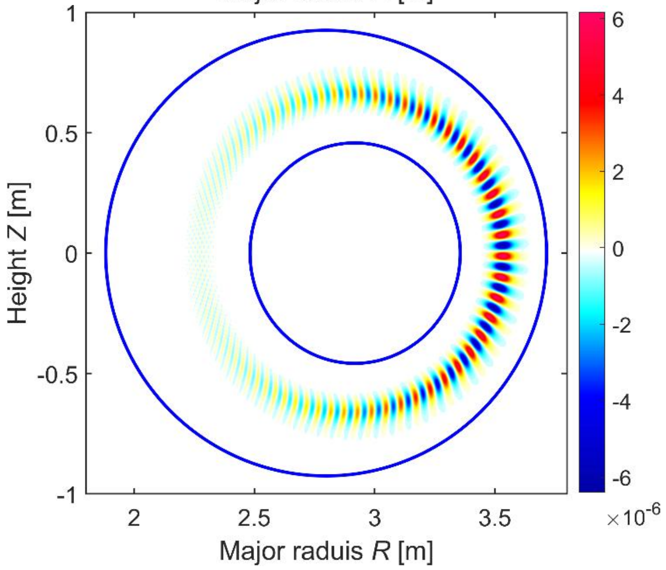

MAS
Eigenvalue approach

J. Bao
2022 NF

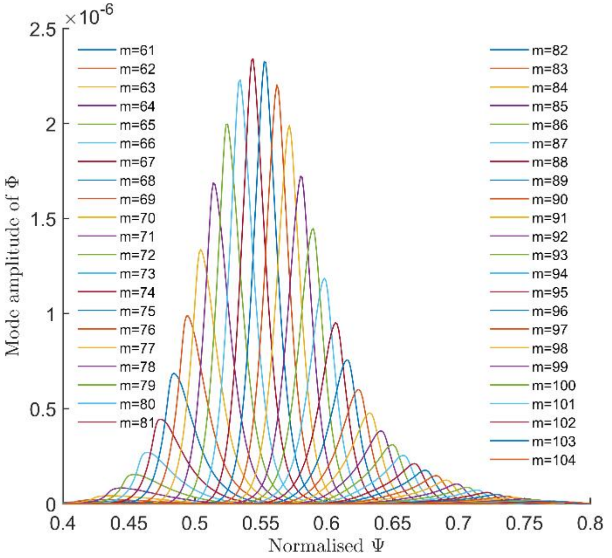

No $\eta_{\parallel}$, no numerical diffusion term

Relative difference with MAS is less than 4%

$n = 20$ Ideal ballooning mode, GMEC costs 15 seconds using 448 cores.

Benchmark with MAS: diamagnetic drift effects

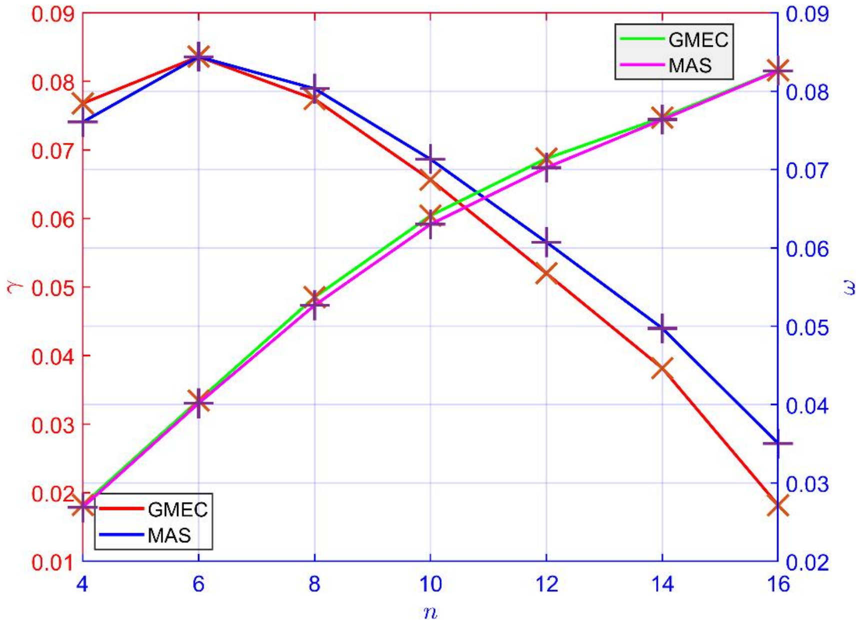

Relative differences for ω are less than 1% and those for γ are about 10%

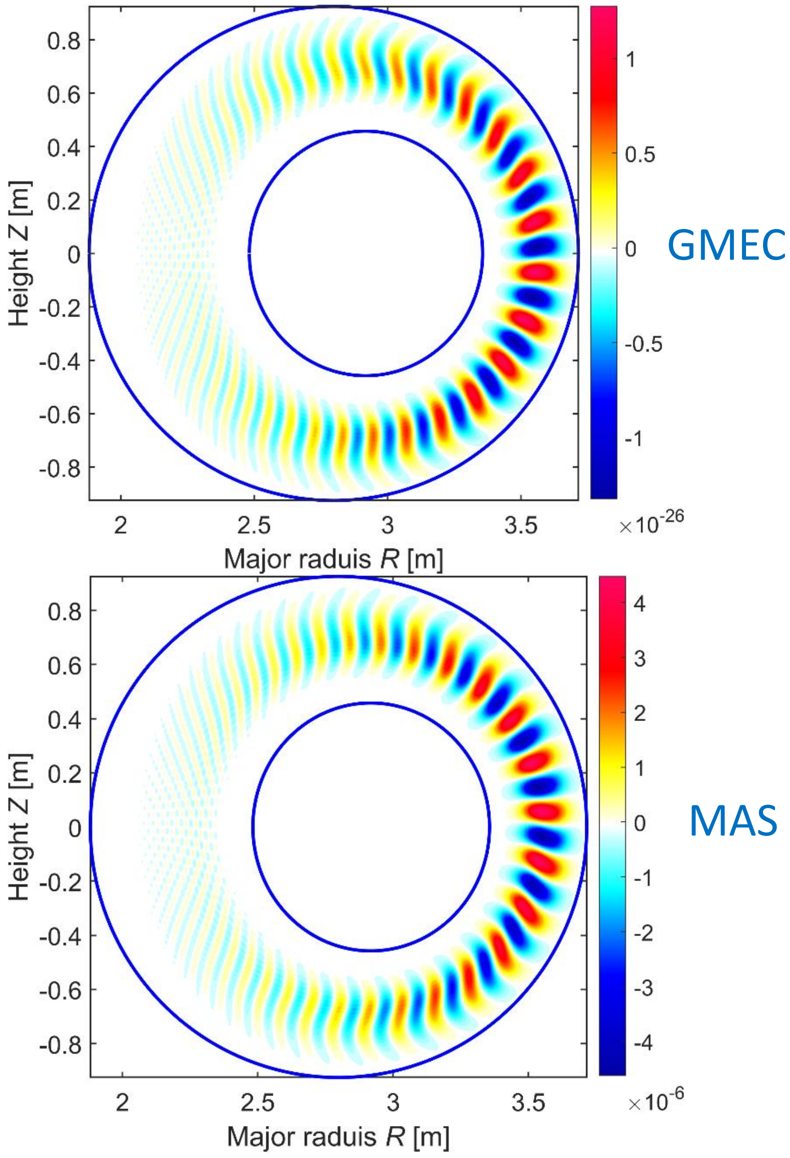

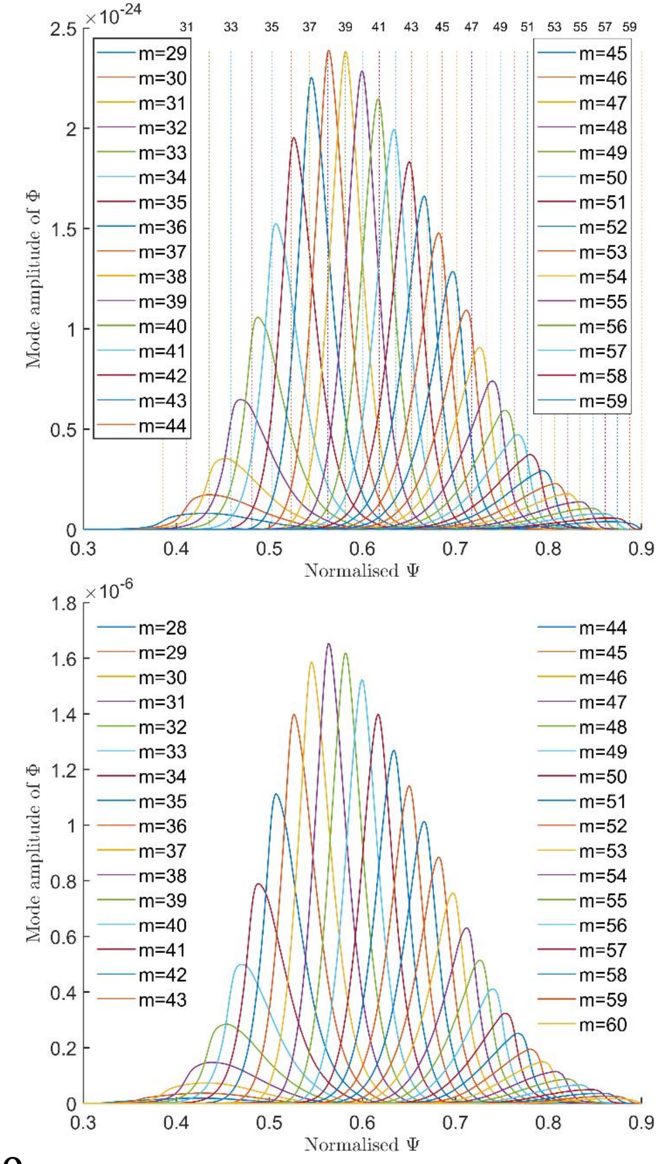

$n = 10$

Benchmark with MAS: tearing mode

$m/n = 2/1$ tearing mode

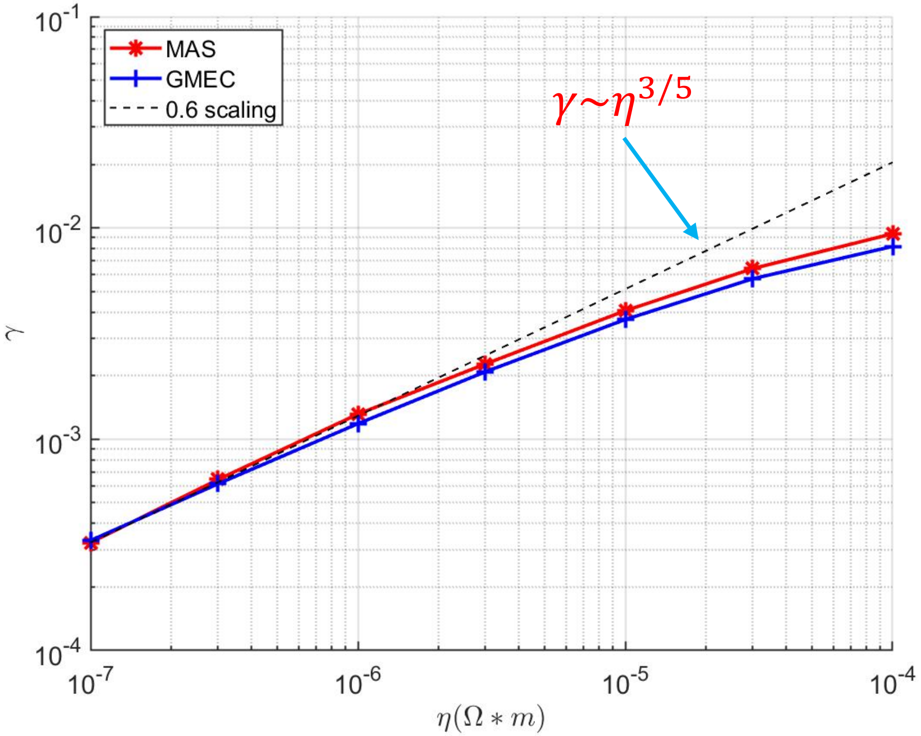

Relative differences with MAS are less than 15%

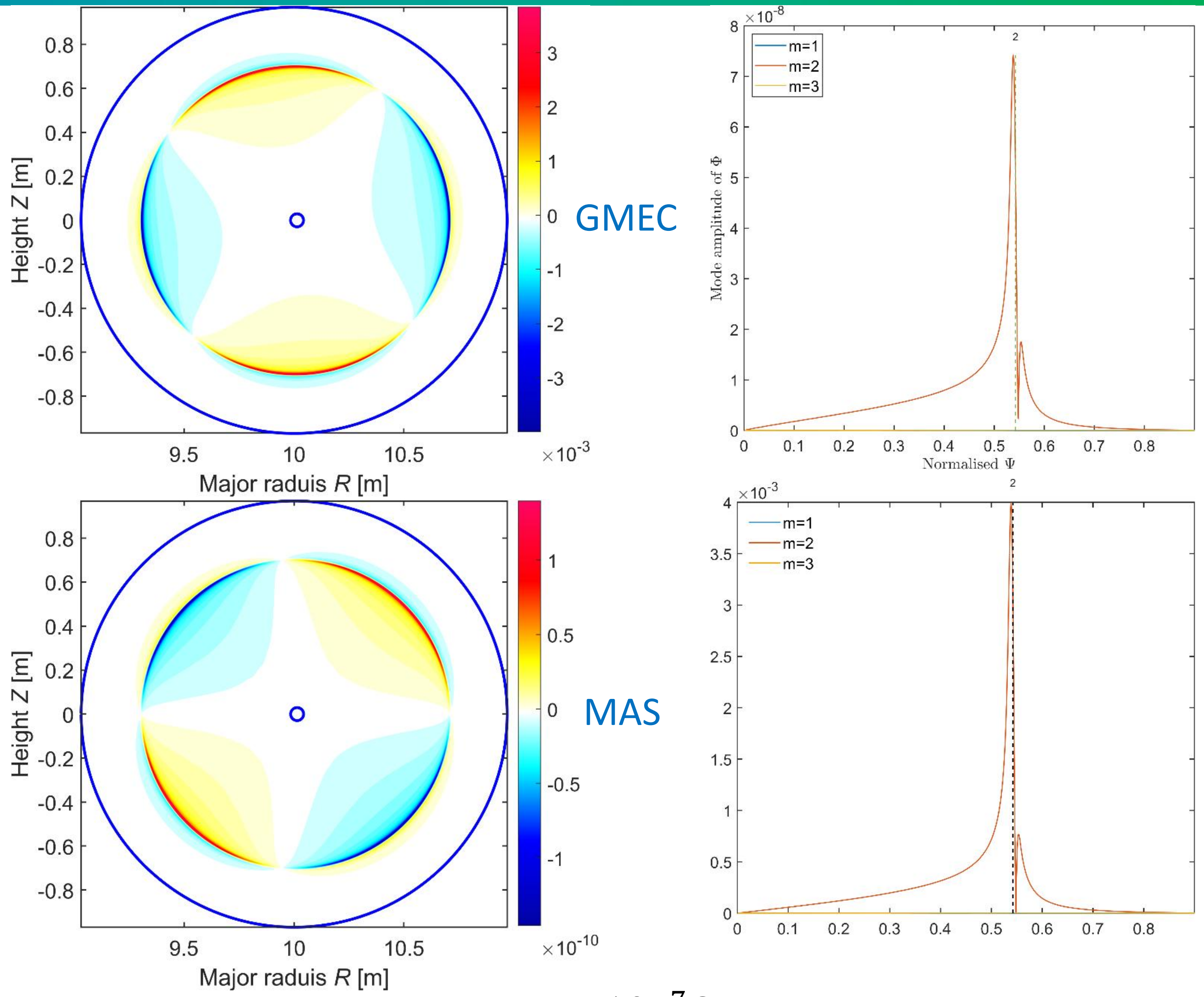

$\eta = 10^{-7}\Omega \cdot m$

Verification of single particle orbits in equilibrium magnetic field

Zhaoyang Liu

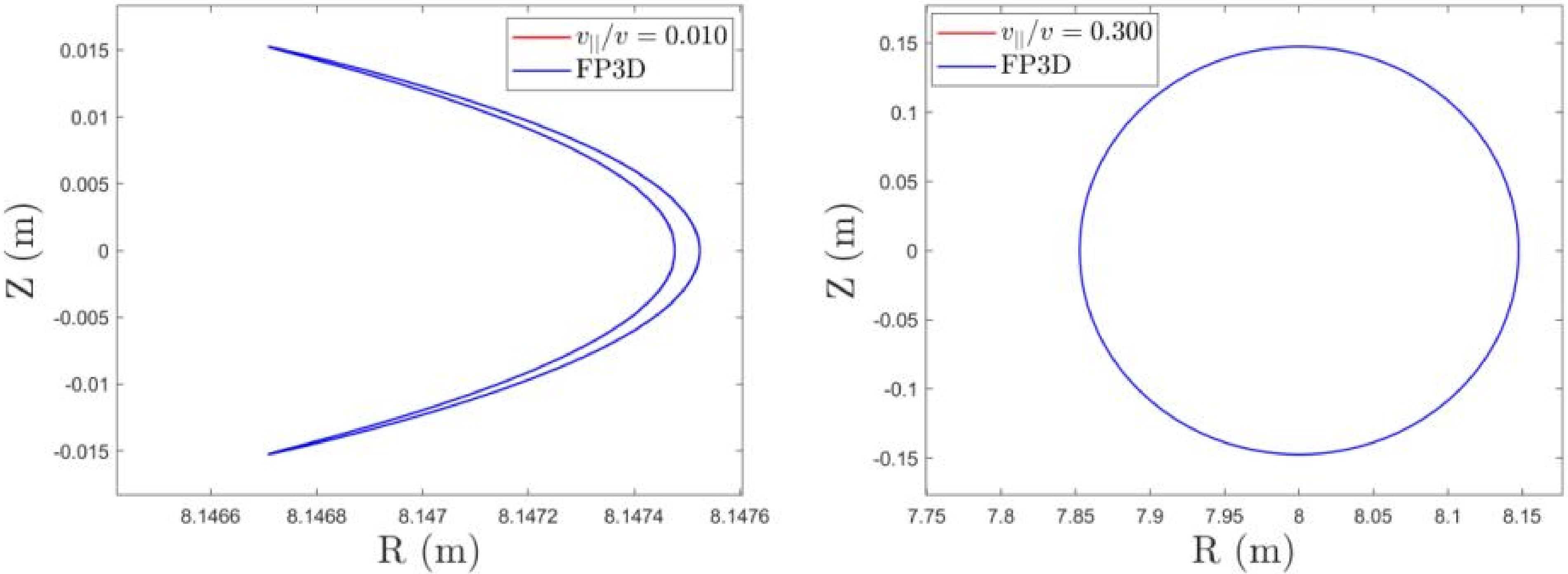

图 1.5：粒子能量 $E = 1\mathrm{eV}$，速度 pitch 角 $v_{||}/v = 0.01,\ 0.3$ 的粒子轨道

Verification of Single Particle Orbit in Equilibrium Magnetic Field

Zhaoyang Liu

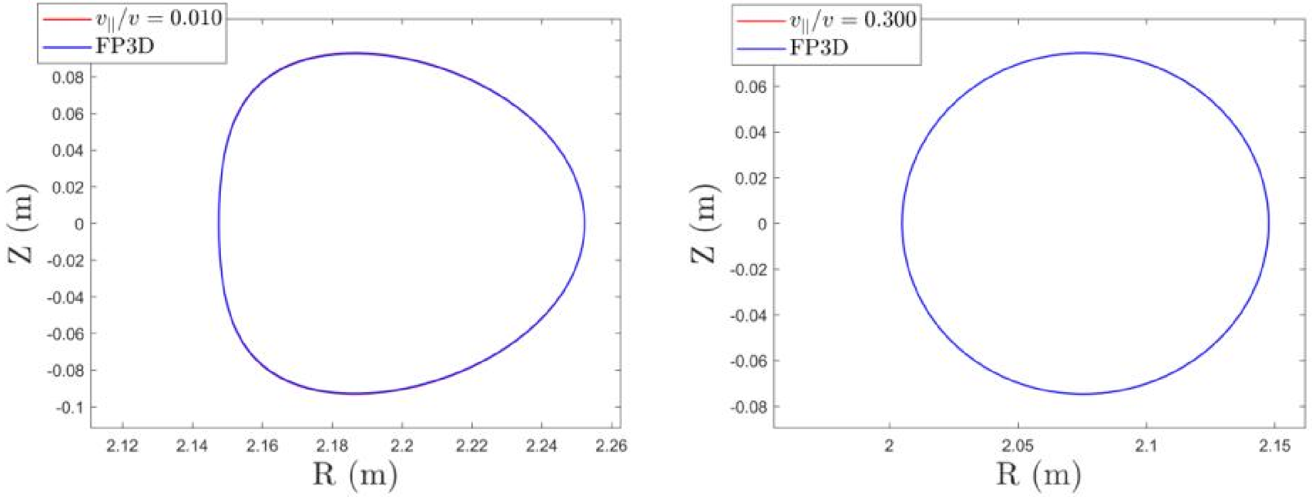

图 1.7：粒子能量 $E = 1\text{MeV}$，速度 pitch 角 $v_{||}/v = 0.01,\ 0.3$ 的粒子轨道

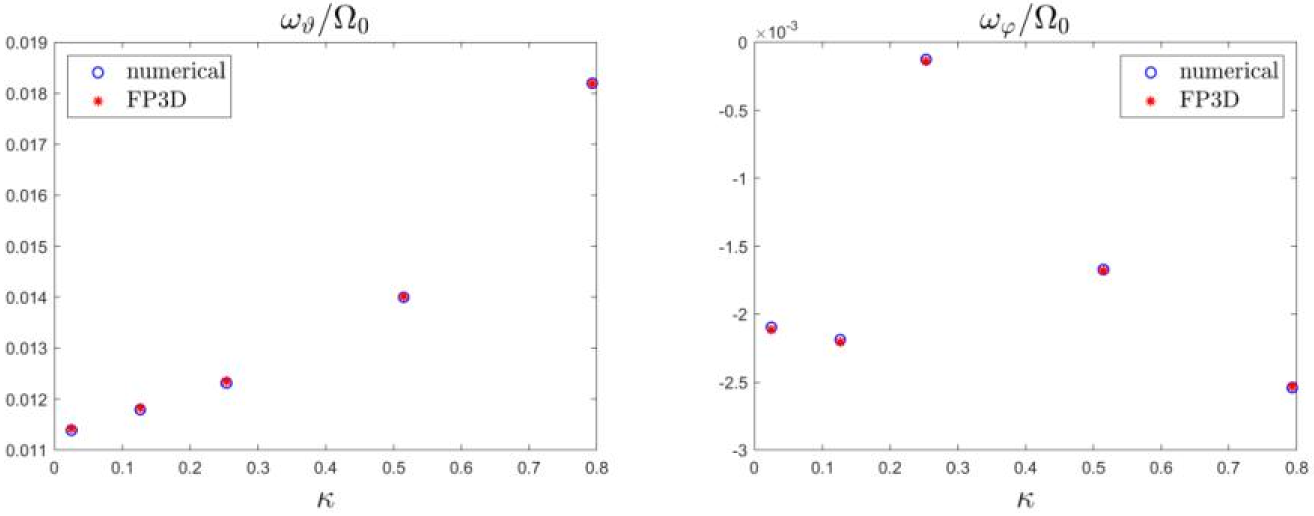

图 1.8：不同 κ 下的粒子轨道宽度，极向运动频率和环向运动频率

Verification of GMEC for an n=3 TAE with a circular tokamak equilibrium

Zhaoyang Liu

- Equilibrium parameters $R_0 = 3\mathrm{m}$, $a_0 = 1\mathrm{m}$, $B_0 = 1\mathrm{T}$,

  $\psi_1 = 0.01$, $\psi_2 = 1$, $n(\psi) = 1$, $P(\psi) = 0$,

  $q(\psi) = a_0 + a_1\psi + a_2\psi^2$, $a_0 = 1.6667$, $a_1 = 0.5$, $a_2 = 0.8333$。

- EP parameters $M = 1$, $Q = 2$, $v_{\max} = 2v_{A0}$, $\rho_{\max} = 0.072\mathrm{m}$, $v_c = 0.58v_{\max}$。

$$f_0(E, P_\varphi) = \frac{cH(v_{\max} - v)}{v^3 + v_c^3}\exp\left(-\frac{\psi}{0.25}\right), \quad \beta_h = 0.02。$$

- Numerical grids (1/3 torus for n=3 mode) $n_x = 256$, $n_y = 64$, $n_z = 16$。

- 32MPI×28Threads，$\Delta t = 0.1$，20k steps，
  computation time：0.4 hour on the Tianhe supercomputer

Verification with M3D-K for an n=3 TAE

Φ

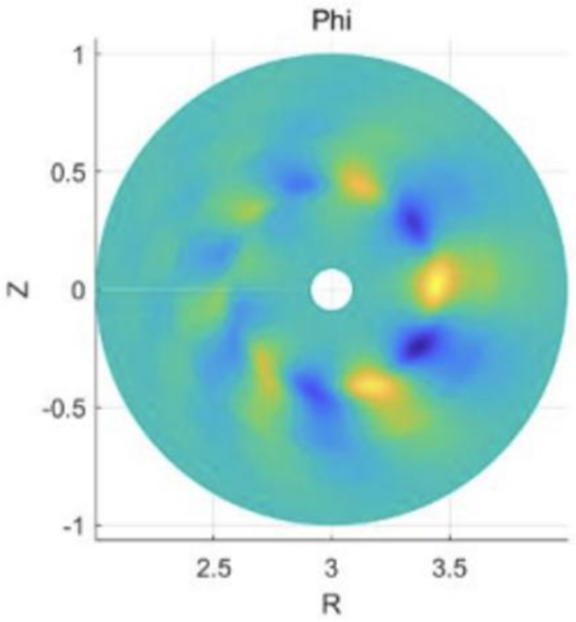

mode frequency

growth rate

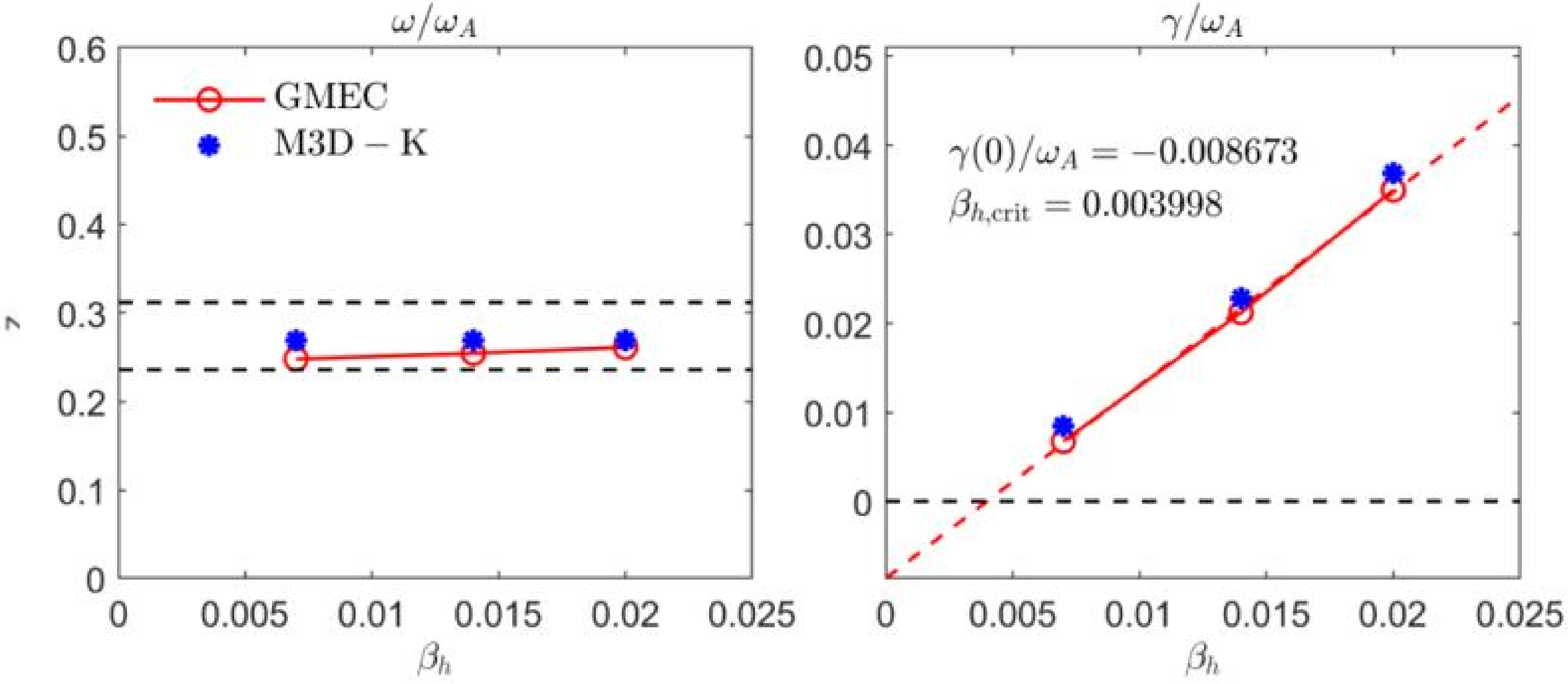

图 1.18：实频率和增长率随高能量粒子 β_h 的变化

Verification of GMEC：RSAEs in DIII-D

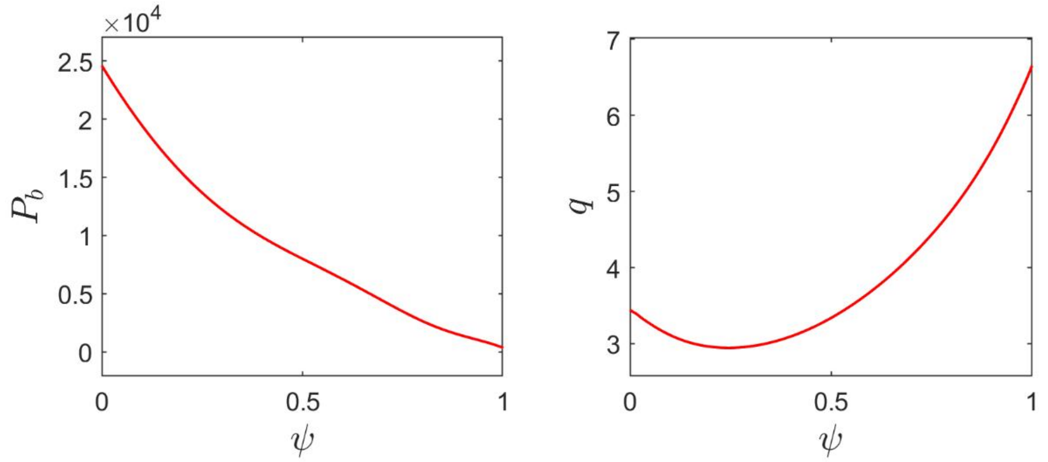

$q_{min} = 3$

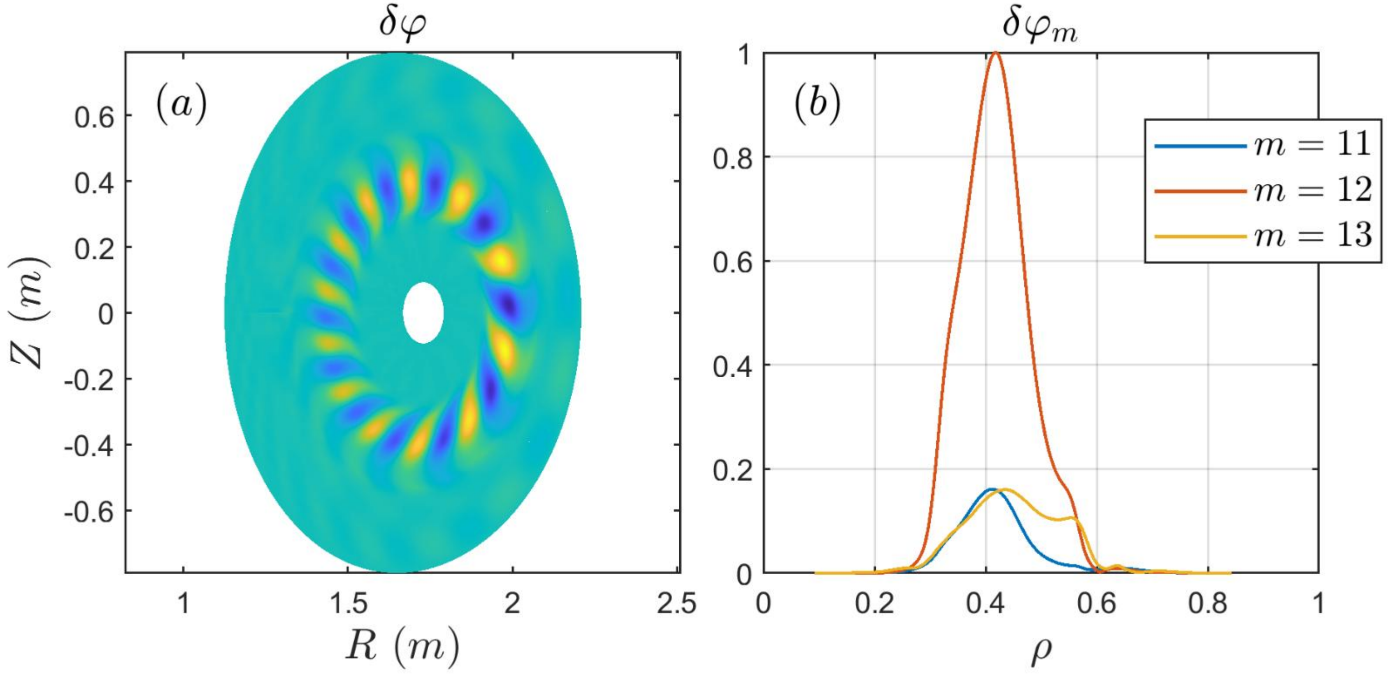

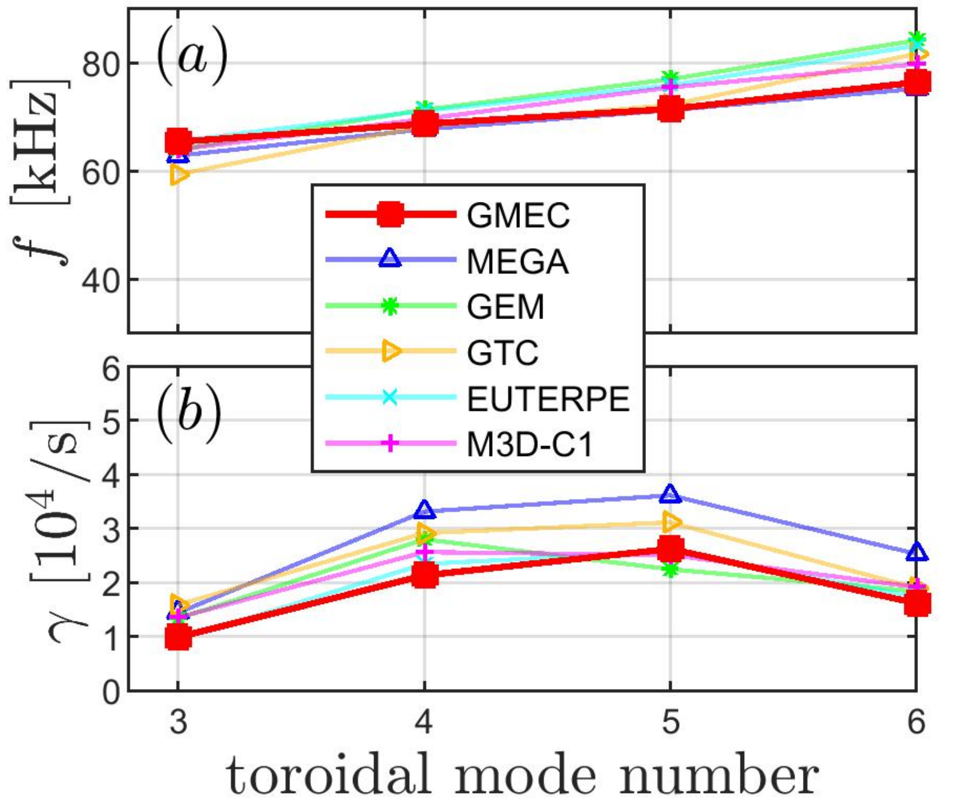

S. Taimourzadeh *et al* 2019 *Nucl. Fusion* **59** 066006

Verification of GMEC：n=6 TAE

A TAE mode with m = 10, 11 and n = 6 is calculated in a hydrogen plasma

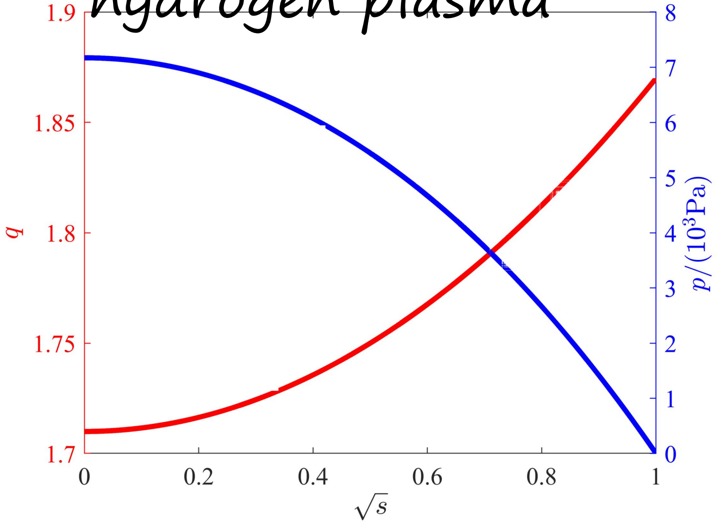

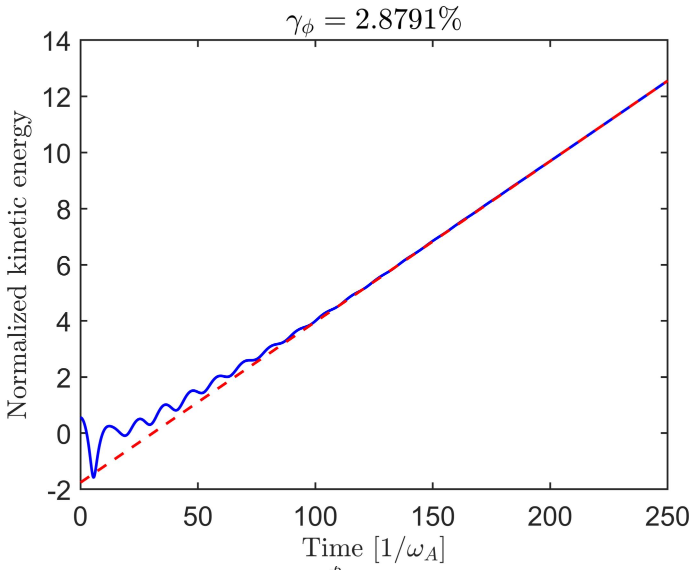

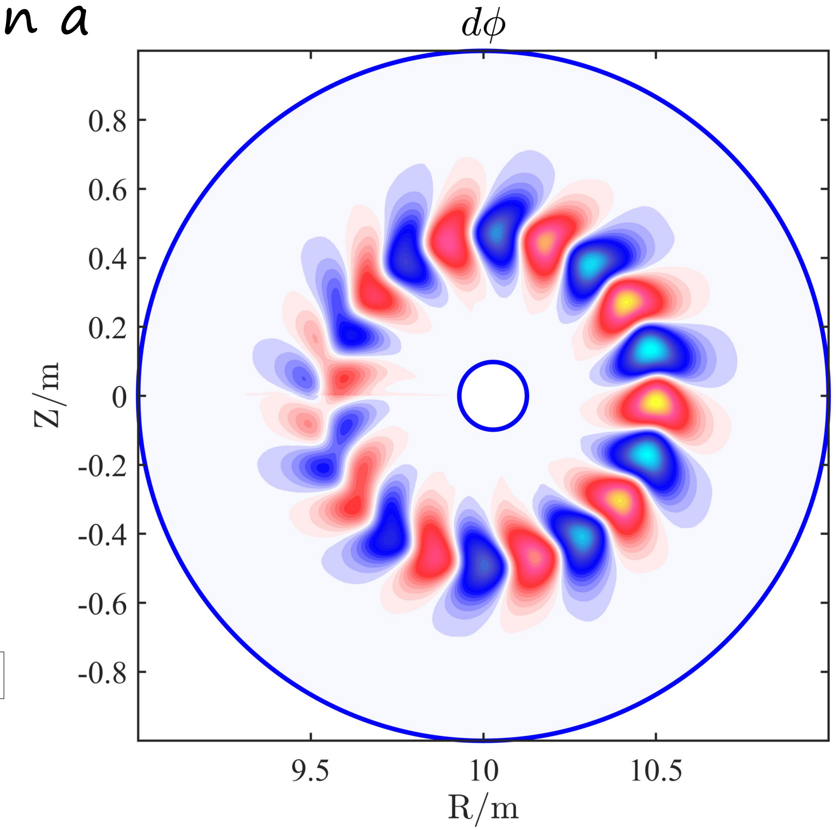

$$n(s) = n_0 c_3 \exp\left(-\frac{c_2}{c_1}\tanh\frac{\sqrt{s}-c_0}{c_2}\right)$$

$$n_0 = 1.44131 \cdot 10^{17}\mathrm{m}^{-3}, c_0 = 0.49123$$

$$c_1 = 0.298, c_2 = 0.199, c_3 = 0.521$$

$$R = 10\ m,\ a = 1\ m$$

Maxwellian distribution

A. Könies *et al* 2018 *Nucl. Fusion* **58** 126027

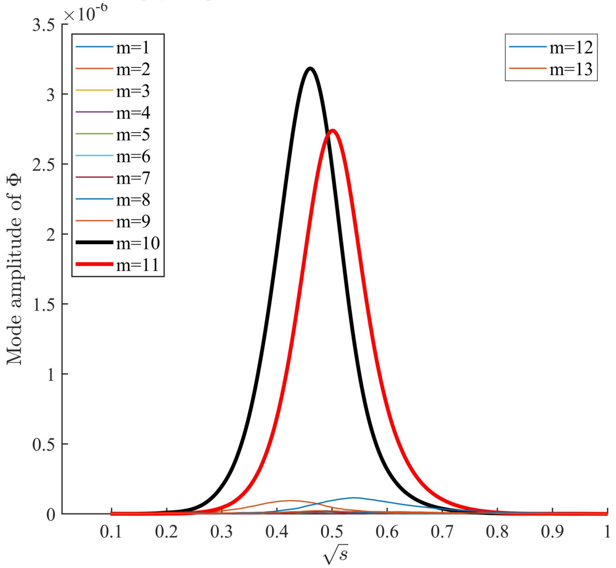

$$(N_x, N_y, N_z) = (256,64,16)$$

$$N_{pc} = 64,\ \ N_{particle} = 16{,}777{,}216$$

$N_{step} = 25{,}000$, $\Delta t = 0.01 R_0/v_A$, RK4

448核, 25 minutes, without FLR

54 minutes, with FLR

Verification of GMEC： n=6 TAE

A. Könies *et al* 2018 *Nucl. Fusion* **58** 126027

wo FLR

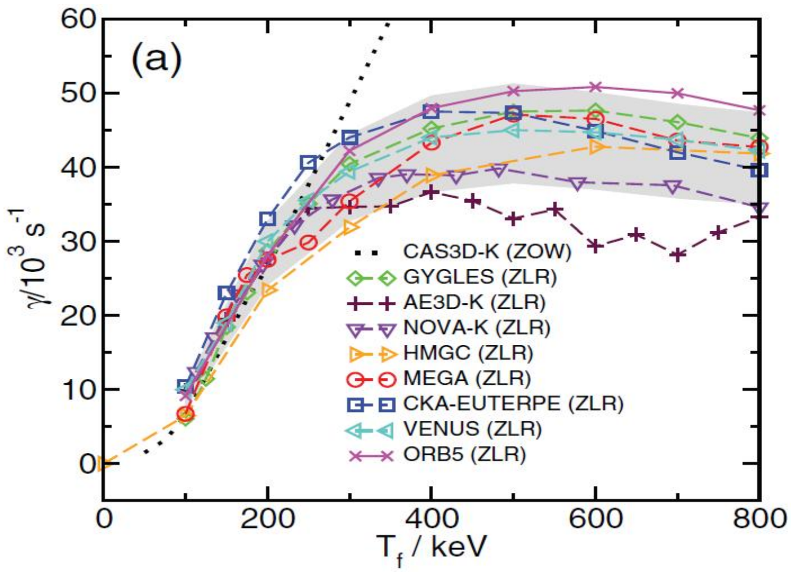

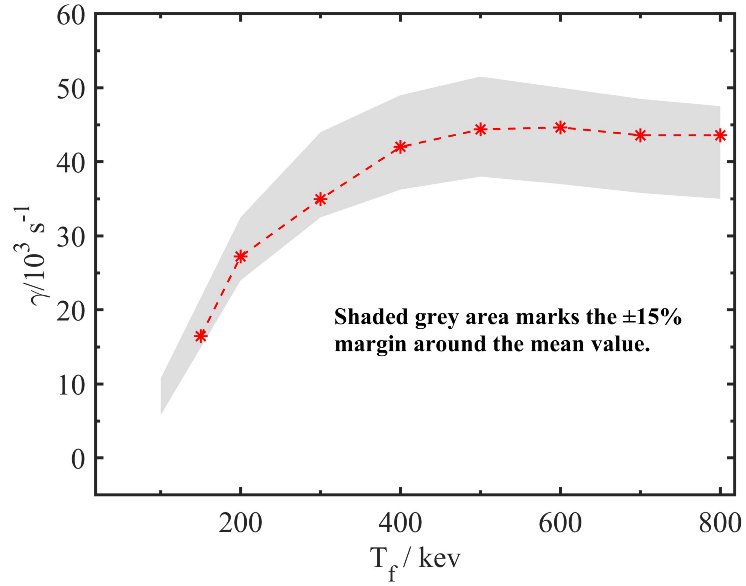

with FLR

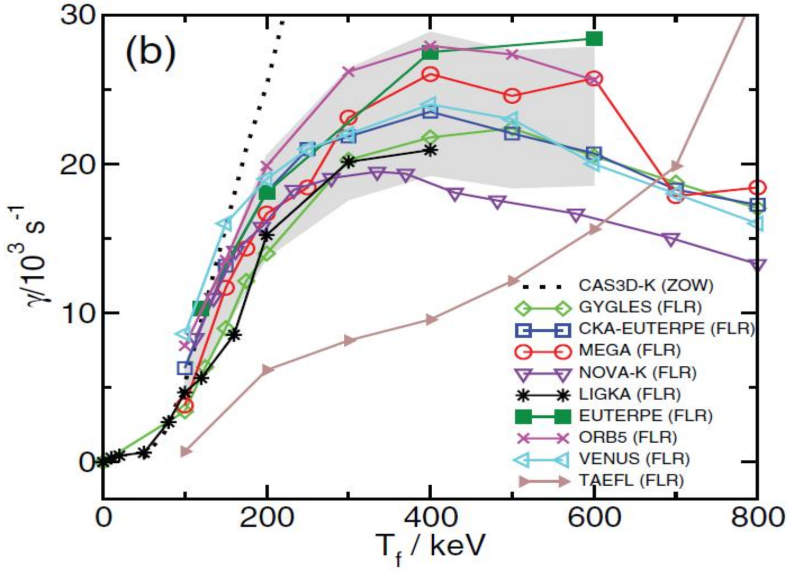

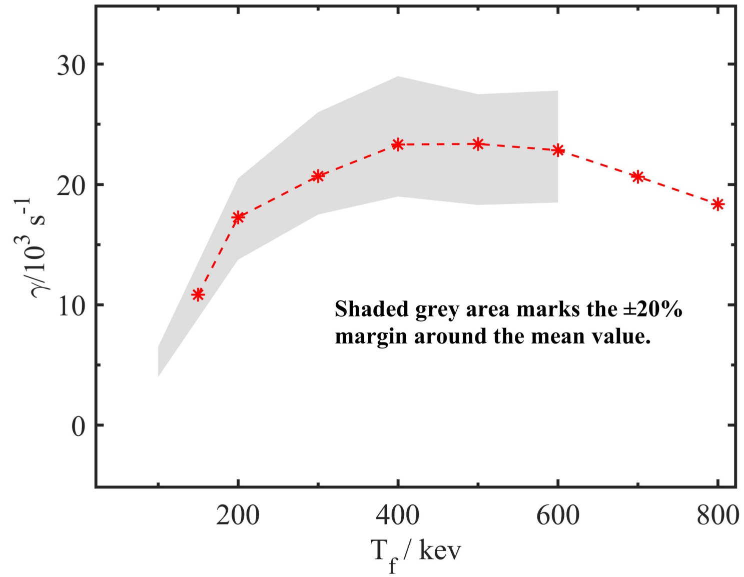

Outline

- Introduction
- Gyrokinetic-MHD Hybrid Model
- Development of GMEC
- GMEC verifications
- GMEC applications
- Summary
- Future Work

Nonlinear results：single n=6 TAE

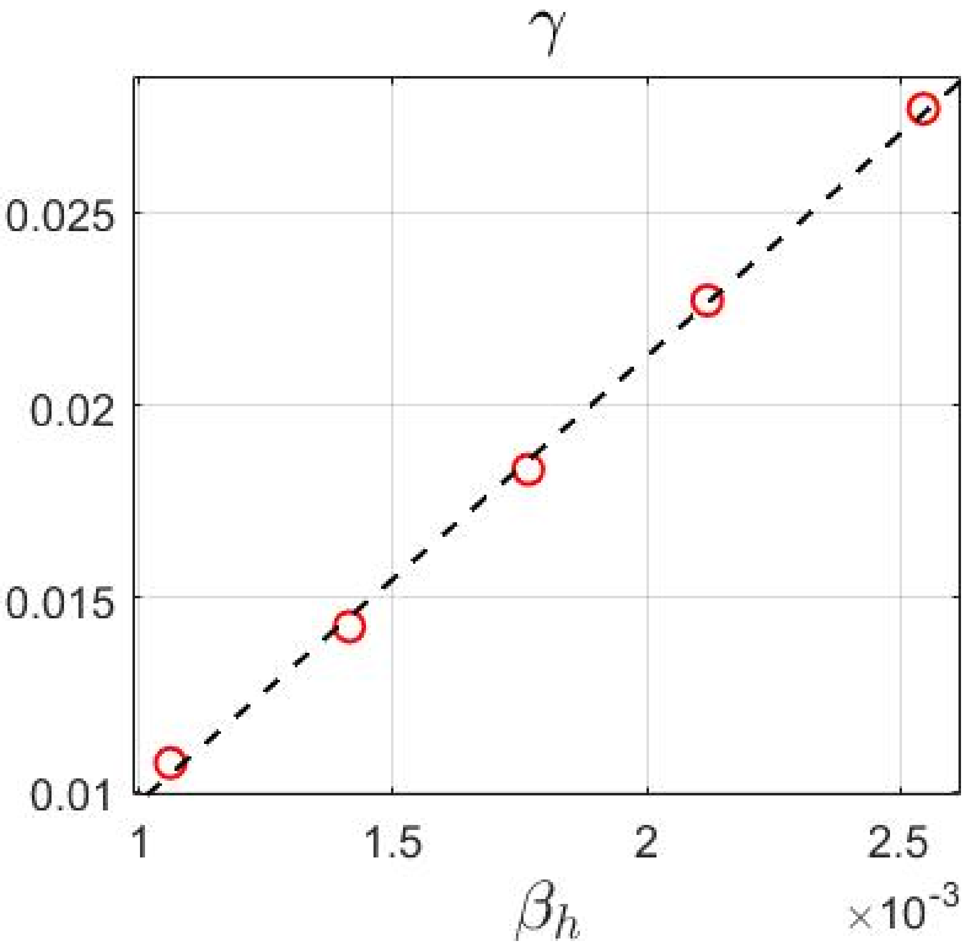

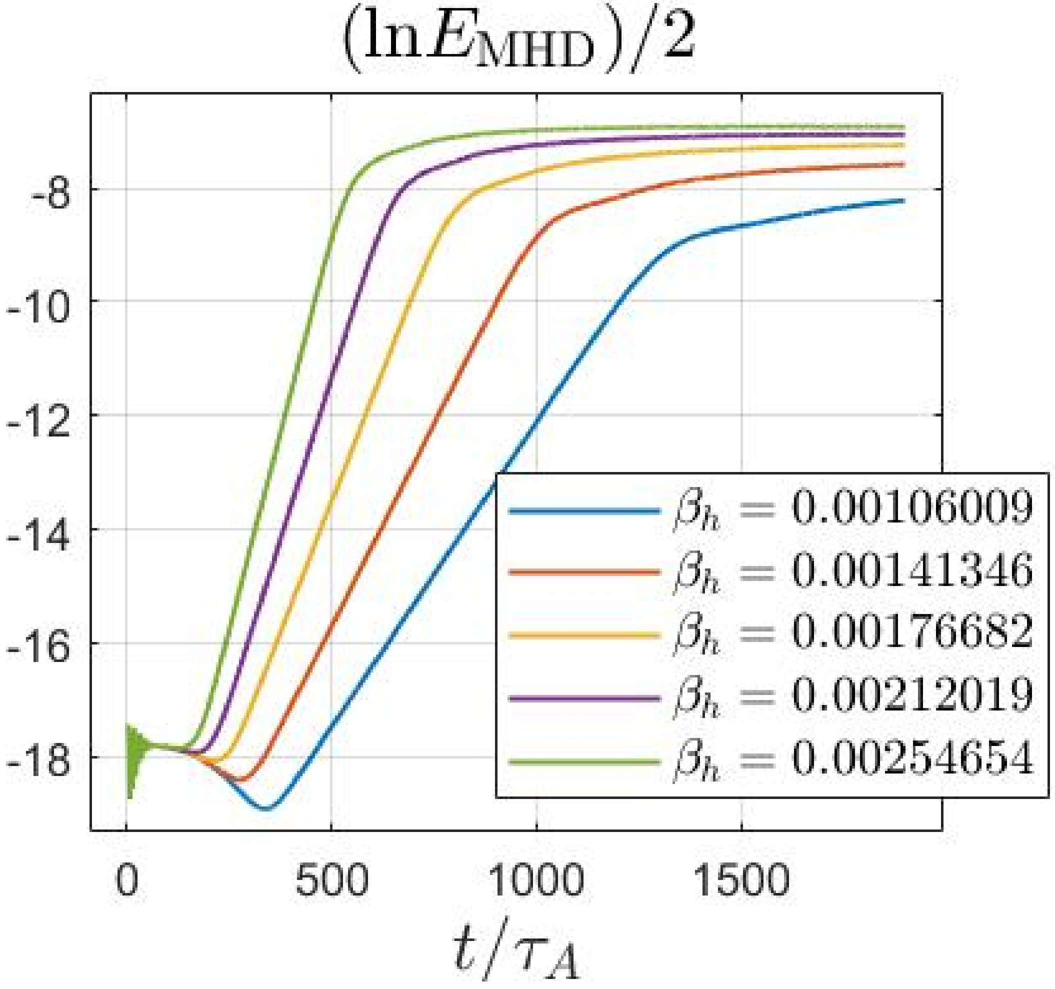

multi-n simulations of the n=6 TAE benchmark case

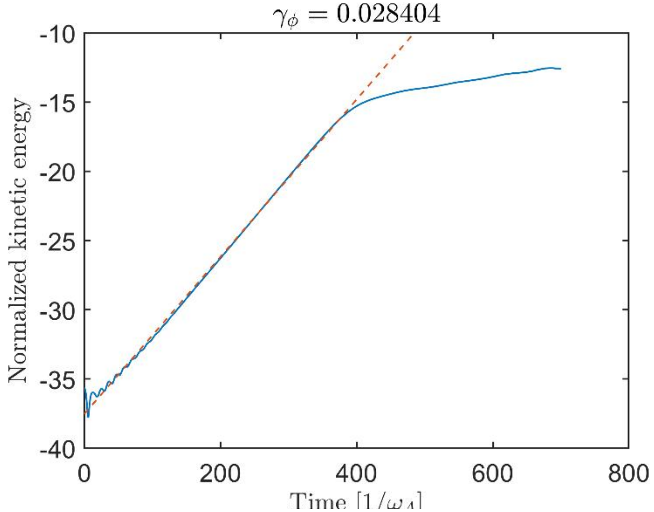

$t = 700R_0/v_A$

Linear phase
$n = 6$

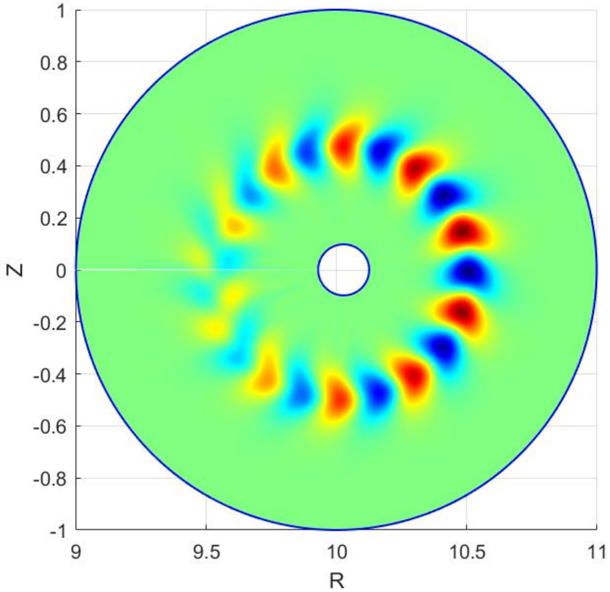

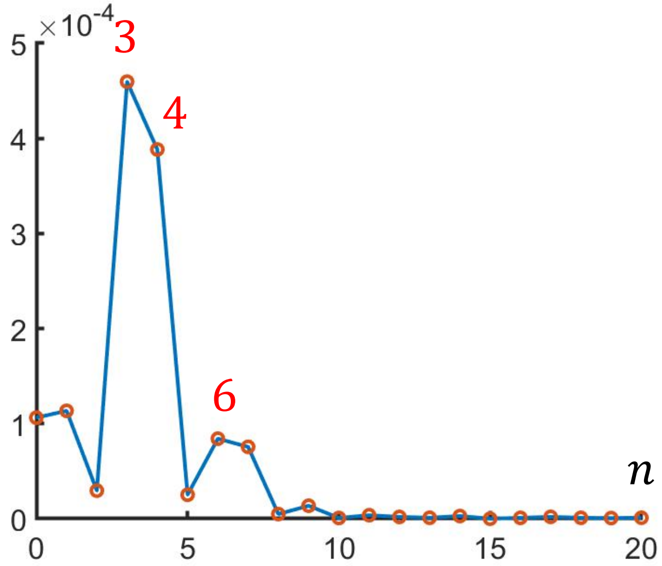

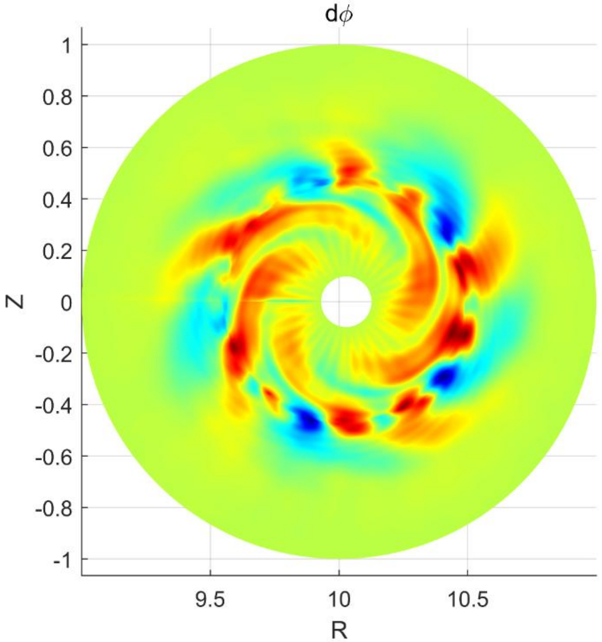

n total

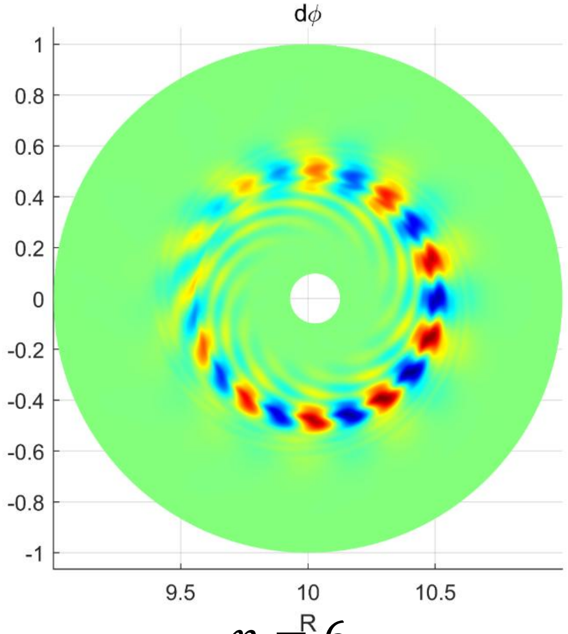

$n = 6$

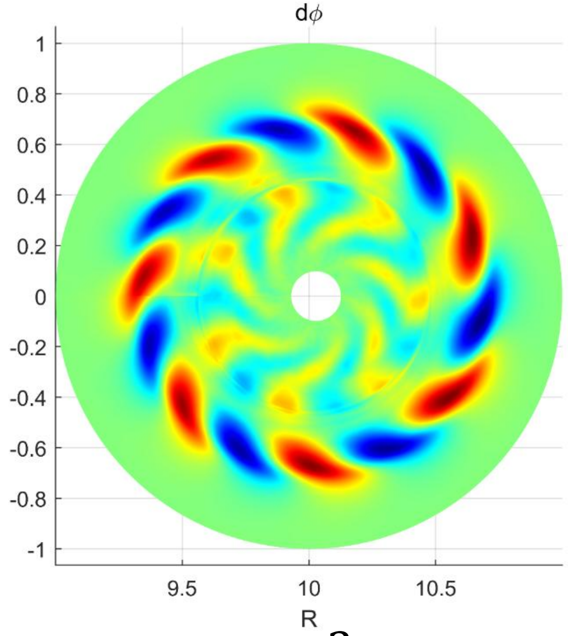

$n = 3$

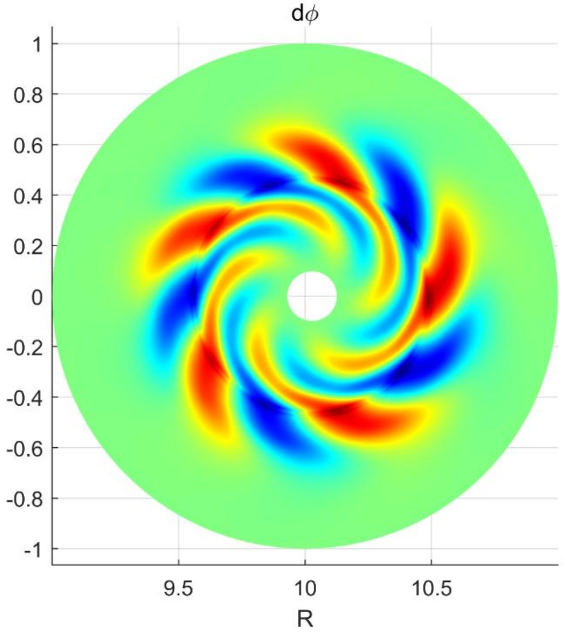

$n = 4$

Nonlinear results： n=4 RSAE in DIII-D

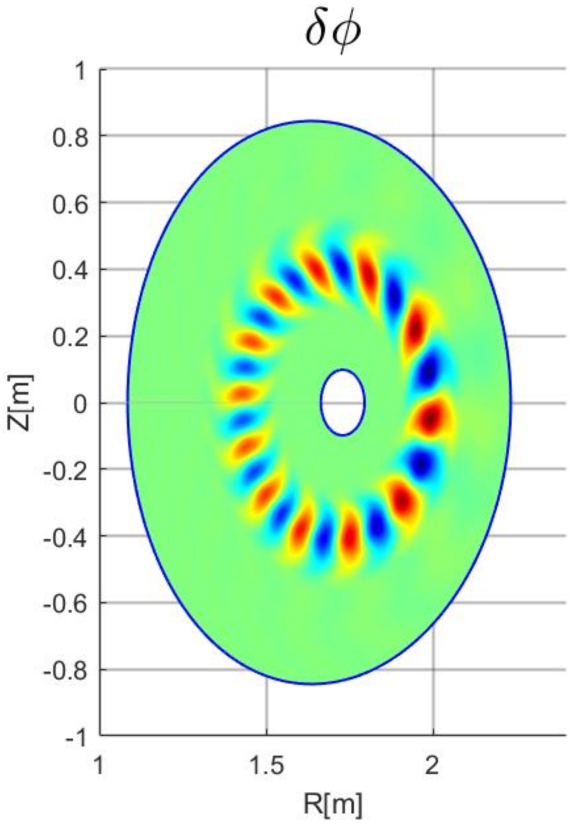

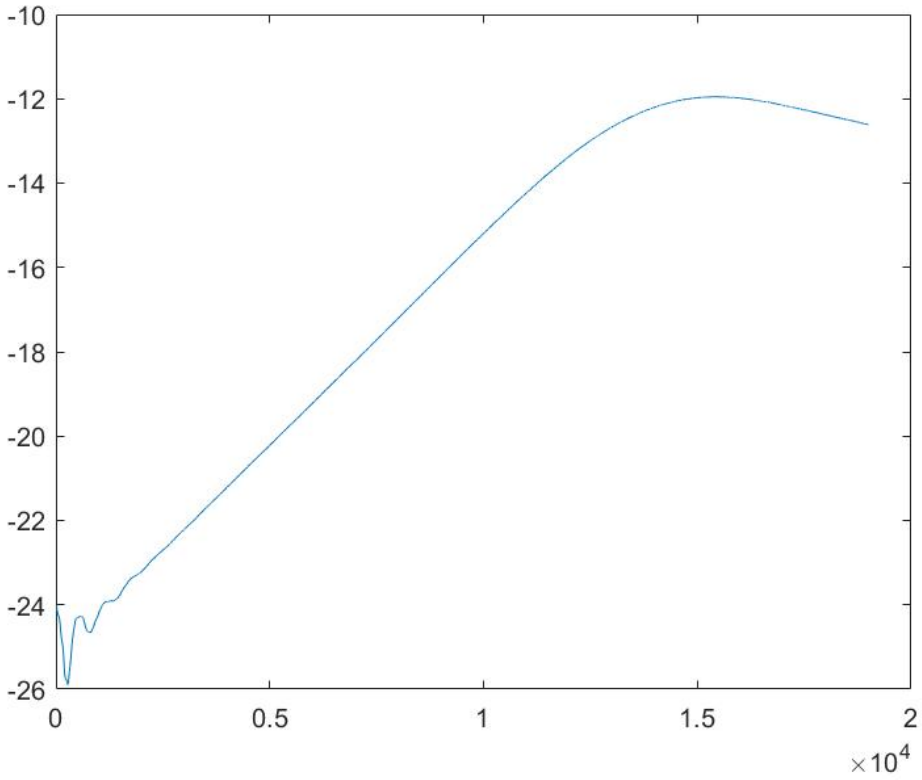

n=10 TAE in CFETR

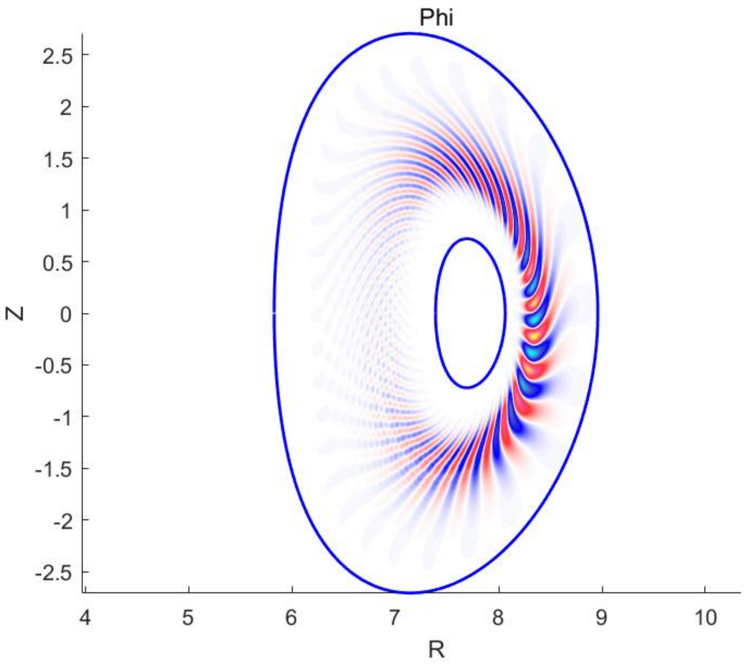

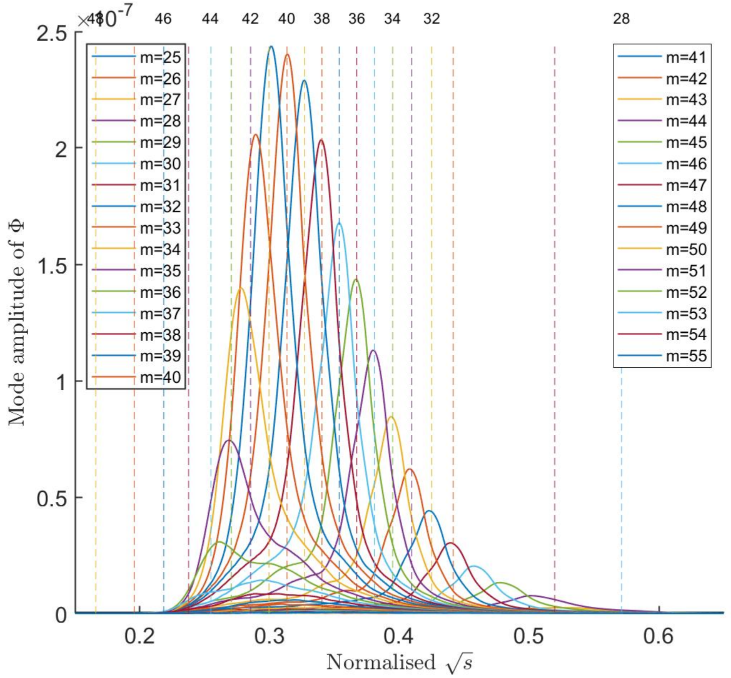

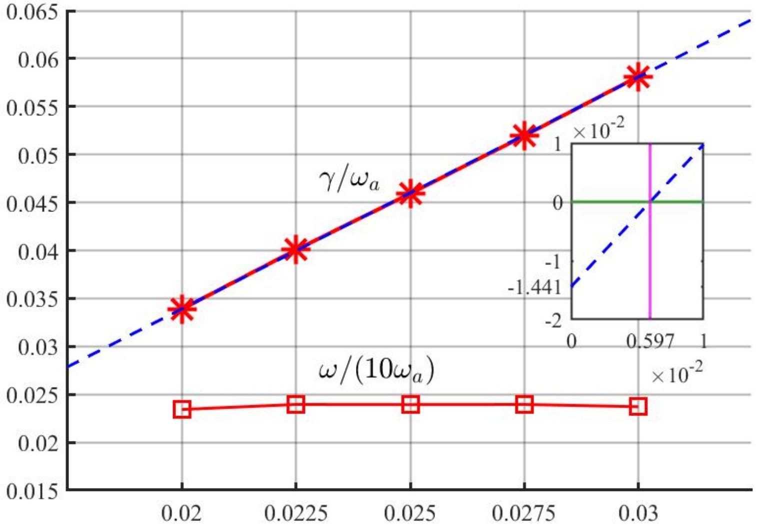

Summary

- An initial version of GMEC has been developed for simulating EP-driven Alfven modes and EP transport in tokamak plasmas. Initial verifications have been done successfully.
- A Compile-time Symbolic Solver (CSS) has been developed to aid the development of GMEC. CSS simplifies the coding greatly with great efficiency and small probability for code errors. It also makes the code easily extensible.
- Initial results indicate GMEC is highly efficient and is significantly faster than existing codes.

Future Work

- Complete the full GMEC model with MHD nonlinearity.
- Applications of GMEC to present tokamak experiments (EAST, HL-3, DIII-D, KSTAR etc) and future burning plasmas;
- Collaborations are welcome for code benchmark and GMEC applications.

MHD part of gyrokinetic-MHD hybrid model (GMEC)

Linearized four-field MHD model

Vorticity equation $$\frac{\partial}{\partial t}\delta\varpi + \vec{v}_{*i}\cdot\nabla\delta\varpi = \delta\vec{B}\cdot\nabla\left(\frac{\mu_0 \mathrm{J}_\parallel}{B}\right) + \vec{B}\cdot\nabla\left(\frac{\mu_0\delta J_\parallel}{B}\right) + \frac{2\mu_0}{B}\vec{b}\times\vec{\kappa}\cdot\nabla_\perp(\delta P + \delta P_h)$$

Ohm's law $$\frac{\partial}{\partial t}\delta A_\parallel = -\partial_\parallel\delta\phi - \eta_\parallel\delta J_\parallel + \frac{P_e}{en_e^2 B}\delta\vec{B}\cdot\nabla n_e + \frac{P_e}{en_e^2}\vec{b}\cdot\nabla\delta n_e$$

Pressure equation $$\frac{\partial}{\partial t}\delta P = -\vec{v}_{E\times B}\cdot\nabla P - \frac{2\Gamma \mathrm{P}}{B}\vec{b}\times\vec{\kappa}\cdot\nabla\delta\Phi$$

Electron density equation $$\frac{\partial}{\partial t}\delta n_e = -\vec{v}_{E\times B}\cdot\nabla n_e$$

where

$$\partial_\parallel = \vec{b}\cdot\nabla \qquad \delta\vec{B} = \nabla\times\left(\delta A_\parallel\vec{b}\right) \qquad P = P_i + P_e$$

$$\delta\varpi = \nabla\cdot\frac{1}{v_A^2}\nabla_\perp\delta\Phi \qquad \delta J_\parallel = -\nabla_\perp^2\delta A_\parallel \qquad \vec{v}_{E\times B} = \frac{1}{B}\vec{b}\times\nabla\delta\Phi \qquad \vec{v}_{*i} = \frac{1}{enB}\vec{b}\times\nabla \mathrm{P_i}$$

Using field-aligned coordinates with the shifted metric method

Equilibrium calculated by VMEC or DESC [D. W. Dudt. 2022 POP]

Boundary Conditions

$$\Phi(\psi,\theta+2\pi,\varphi)=\Phi(\psi,\theta,\varphi),$$

$$\Phi(\psi,\theta,\varphi+2\pi)=\Phi(\psi,\theta,\varphi)。$$

$$\Phi(x,y,z+2\pi)=\Phi(x,y,z)。$$

$$\Phi(x,y+2\pi,z)=\Phi(x,y,z-z_{\text{shift}}),$$

$$z_{\text{shift}}\equiv\int_0^{2\pi}d\theta'\nu(\psi,\theta')。$$

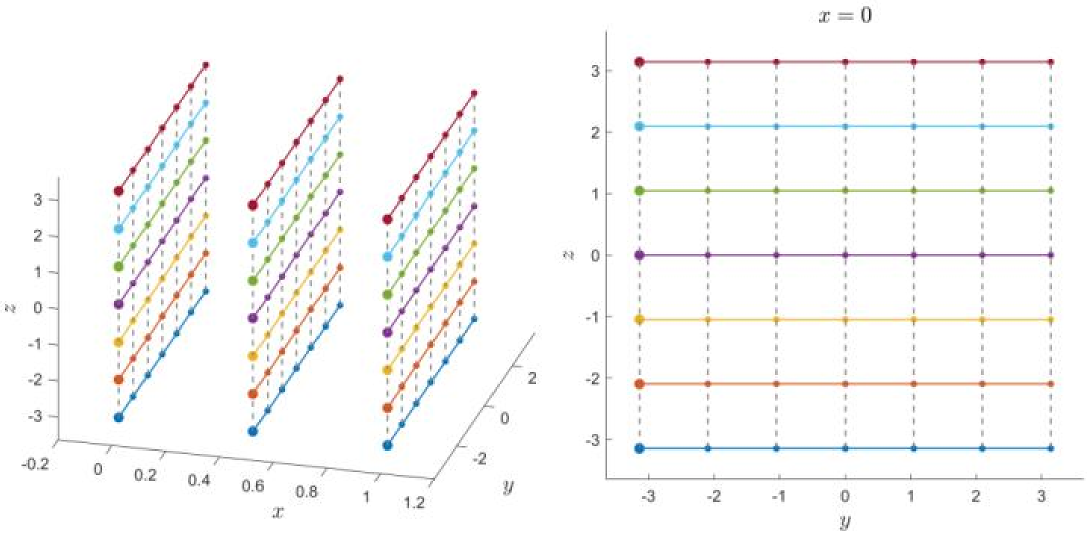

图 1.1：(x,y,z)坐标系中 3×6×6 的三维均匀网格

Gyrokinetic MHD Hybrid Model

- Electrons are described using fluid model;
- Both EPs and thermal ions are described using gyrokinetic model;
- Electromagnetic perturbations are represented by two potentials (electric potential Φ and parallel vector potential $A_{\|}$), thus compressional Alfven waves are not included;
- The system of equations:
  - Gyrokinetic vorticity equations for Φ;
  - Parallel Ohm's law $A_{\|}$;
  - Equation of state for electron pressure;
  - Gyrokinetic equations for distribution of thermal ions and Eps .